Supplementary Document of "A Knee Point Driven Evolutionary Algorithm for Multiobjective Bilevel Optimization"

Jiaxin Chen, Jinliang Ding, *Senior Member, IEEE,* Ke Li, *Senior Member, IEEE,* Kay Chen Tan, *Fellow, IEEE,* and Tianyou Chai, *Life Fellow, IEEE*

I. Appendix A

In this section, we first give a detailed description of the test problems proposed by us. Then, we give the characteristics and formulas of the test problems used in the comparison with the classical methods. After that, a practical problem is presented, including the background, process flow, and mathematical formula. Thereafter, we delineate the experimental setup of the algorithms.

A. Benchmark Test Problems

We propose a series of multiobjective bilevel optimization test problems based on the bottom-up [1] and multiobjective bilevel optimization construction principles [2]. The proposed test problems (dubbed MBOP12 to MBOP15) are built on single-level test problems DEB2DK, DO2DK from [3], and DEB2DK2, DEB2DK1 from [4]. MBOP12 to MBOP15 present various difficulties to the multiobjective bilevel optimization, such as scalable, and discontinuity. The mathematical formulas and corresponding parameters are given in Table I.

MBOP12 is designed based on MBOP1 and DEB2DK. It features a complicated lower-level Pareto front (PF) shape and upper-level optimal solution solving procedure. Additionally, MBOP12 is a continuity, convexity, and scalable multiobjective bilevel test problem. For different upper-level decision variables, the lower-level Pareto-optimal solutions are located in $f_1^{\mathrm{L}}(\mathbf{x}) = q(x_1^{\mathrm{L}})\sin(\frac{\pi x_1^{\mathrm{L}}}{2})$, $f_2^{\mathrm{L}} = q(x_1^{\mathrm{L}})\cos(\frac{\pi x_1^{\mathrm{L}}}{2}) - x_1^{\mathrm{U}}$. For every $i = 2, \cdots, K$, $x_i^{\mathrm{L}} = x_i^{\mathrm{U}}$. Parameter β in $q(x_1^{\mathrm{L}})$ controls the number of knee points in the lower level and is set to 4. For the upper-level problem, since the dominance relationship, the optimal solution is located on the lower left quarter circle with the center of $(1 + r, 1 + r)$ and the radius of 1.

MBOP13 presents a challenging discontinuity problem within the realm of multiobjective bilevel optimization, characterized by a difficult constraint. This test problem draws inspiration from the single-level DEB2DK2 test problem. For the lower-level problem, $x_j^{\mathrm{L}} = 0$, for $j = K + 1, \ldots, K + L$, and the Pareto-optimal solution is located in $f_1(x) = r(x_1^{\mathrm{L}})\sin^3(\frac{\pi x_1}{2})$, $f_2(x) = r(x_1^{\mathrm{L}})\cos(\frac{\pi x_1}{2})$. But not all the solutions in the lower-level reaction set are in the inducible region because of upper-level constraint $G(\mathbf{x}^{\mathrm{U}}, \mathbf{x}^{\mathrm{L}})$. We set the parameter controlling the number of knee points β as 2, and the upper-level problem has a discontinuous front, that is, the part where the PF of DEB2DK2 meets the constraint $G(\mathbf{x}^{\mathrm{U}}, \mathbf{x}^{\mathrm{L}})$. Besides, $x_j^{\mathrm{L}} = 0$ for $j = 2, \ldots, K + L$.

MBOP14 is a discontinuity problem designed based on the shape of DO2DK. In this problem, we add some difficulty to the solving procedure of the upper-level problem by setting the function $T(t_1(\mathbf{x}), t_2(\mathbf{x}))$. Through filtering some lower-level solutions, only part of the solutions can be the candidate for the upper-level optimal solutions. Thereby, examining the performance of the algorithm. For the upper-level PF, $x_j^{\mathrm{U}} = 0$, for $j = 2, \ldots, K$, and satisfies the function $f_1(\mathbf{x}) = r(x_1^{\mathrm{L}})\big[\sin(\frac{\pi x_1^{\mathrm{L}}}{2^{s+1}} + (1 + \frac{2^{s-1}}{2^{s+2}})\pi) + 1\big]$, $f_2(\mathbf{x}) = r(x_1^{\mathrm{L}})\big[\cos(\frac{\pi x_1^{\mathrm{L}}}{2} + \pi) + 1\big]$, in the part of $z(x_1, x_2)$ region.

The test problem MBOP15 is deceptive and is constructed using the format of DEB2DK1. In this problem, we set τ_1 and τ_2 to positive numbers, which indicates that the solutions not in the feasible region may obtain a smaller upper-level function value than the true optimal solution. However, these solutions are not feasible according to the definition of bilevel optimization. This structure makes this problem difficult to solve. To prevent the algorithm from jumping into the undesired areas at the beginning, we use a progressive value $T(x_1, x_2)$ to make the algorithm try to find a feasible solution. The upper- and lower-level optimal solutions are the intersection of the function ($f_1(\mathbf{x}) = r(x_1^{\mathrm{L}})\sin\frac{\pi x_1^{\mathrm{L}}}{2}$, $f_2(\mathbf{x}) = r(x_1^{\mathrm{L}})\cos\frac{\pi x_1^{\mathrm{L}}}{2}$) and region $z_1(x_1, x_2)$.

B. Test Problems Used in Comparison to Classical Methods

To compare our proposed algorithm `TKDEA` with classical methods, we compare it with some classical methods. We first compare `TKDEA` with the classical methods proposed in [5] and [6] on the test problem in [6]. For convenience, the test problem and the two algorithms are dubbed Classic1, `CA1`, and `CA2`, respectively. `CA1` is a classical method that is used to address linear multiobjective bilevel optimization problem (MBLOP). The main idea of `CA1` is to use a Pareto-filter scheme to find an approximated discrete representation of the efficient set. `CA2` could solve the linear MBLOP where the constraint regions of the upper level and lower level be non-empty and compact. It uses fuzzy set theory and fuzzy programming to convert the linear multiobjective bilevel programming problem to a linear bilevel programming problem, then extends the Kth-best method to solve the final linear bilevel programming problem.

Then we compare TKDEA with the classical method (dubbed CA3) in [7]. We test the two algorithms on the test problem used in [7] (dubbed Classic2), which is also known as TP3 [2], [8]. CA3 is a classical method that assumes some restrictions as bicriteria problems on both levels and a one-dimensional upper-level variable. It works on nonlinear non-convex MBLOPs. The detailed test problem formulations are given in Table II.

C. Petroleum Refining Problem

To validate the effectiveness of our proposed algorithm, we also investigate the performance of TKDEA in a real-world engineering problem.

Petroleum refining is essential for crude oil application, which involves many complex technologies, such as refinery scheduling [9], operational optimization [10], and fast evaluation of physical properties [11]. This energy-intensive process emits a large chunk of greenhouse gases (e.g., carbon dioxide (CO_2)) while splitting crude oil. These greenhouse gases have a significant impact on the global climate and the environment. There are usually two DMs in this practical problem, i.e., the regulating authority and the petroleum refining enterprise. The overall flow chart of the practical petroleum refining MBLOP is given in Fig. 1. The regulating authority acts as a leader and aims to earn revenues through taxes and regulate the environmental damages. On the other hand, the petroleum refining enterprise reacts rationally to the decisions of the leader to maximize its profit and minimize its burnt fuel. The limited non-renewable crude oil resources and rising prices of burnt fuel are forcing the enterprises to achieve their objectives via operational optimization.

Petroleum refining is a huge engineering process that consumes large quantities of energy with many heavy equipments. It is unrealistic to measure all units, and we only study the main unit of petroleum refining, i.e., the crude oil distillation unit (CDU) consisting of an atmospheric furnace (AF) and an atmospheric distillation column (ADC). After the crude oil is partially vaporized, the oil is heated by the AF and enters the ADC. The ADC consists of a main column, a condenser, three side-draw product strippers, and three pumparounds. The flashed feed vapors move upwards from the flash zone in the ADC, and the liquid moves downwards from the top to the bottom of the column due to gravity. The high-temperature gas and the low-temperature liquid meet at the tray for partial condensation and partial vaporization. The oil is cut off at different boiling points by this physical method. The top distillate product is naphtha, and the side-draw products from the three steam strippers are kerosene, light diesel, and atmospheric gas oil (AGO).

In terms of environmental preservation, heating and steam furnaces are one of the main sources of CO_2. The mathematical formulas for calculating the amount of fuel burnt and CO_2 emission are taken from [12]. In this petroleum refining MBLOP, there are two assumptions. One is that the heat duty required by the furnace is proportional to the yield of the crude oil and product flow rate. The second is that the steam heat duty is proportional to the steam flow rate. The CO_2 emission and the tax revenue of the regulating authority form the upper-level constraints. The lower-level constraints mean the overall product flow rate cannot exceed the oil flow rate, and the petroleum refining enterprise must obtain a certain income. This NP-hard problem is difficult to solve in a straightforward way. The formulation of the petroleum refining problem is given in Table III. Some notations are used in the practical petroleum refining MBLOP. The summary of notations and their values are given in Table IV.

D. Parameter Setting

The parameter setting of the experiment is given in Table V. N^{U} and N^{L} are the sizes of upper- and lower-level populations, respectively. T^{U} and T^{L} are the generations of upper- and lower-level problems, respectively. Since the complexity of BLEMO is $O(N^{\mathrm{U}}(2T^{\mathrm{U}}+1)(T^{\mathrm{L}}+1))$, and TKDEA algorithm complexity is $O(N^{\mathrm{U}}(T^{\mathrm{U}}+1)(T^{\mathrm{L}}+1))$. For the sake of fairness, the overall number of function evaluations should be kept as consistent as possible. Thus, the generation of the upper-level problem of BLEMO is set to be $T^{\mathrm{U}}/2$. To eliminate any side effects brought the non-Pareto-optimal solutions or deceptive solutions, the solutions dominate the PF at the upper-level are removed from the HV calculation. In particular, the ideal and nadir points of each benchmark test problem are given in the seventh and eighth column of Table V.

The dimensions of upper- and lower-level decision variables are listed in the sixth column of Table V in the form of $(n_{\mathrm{u}}, n_{\ell})$, where n_{u} and n_{ℓ} represent the dimension of decision variables at the upper level and lower level. For MBOP1–MBOP3 and MBOP12, K is set to be 3. For MBOP4, MBOP5, MBOP6, MBOP7, MBOP13, and MBOP15, two parameters control the dimension of the variable, where K is set to be 3, and L is set to be 2. For MBOP14, K is set to be 5. For the scalable MBOP9 test problem, the values of K are set to 2, 6, and 14, dubbed MBOP9-K2, MBOP9-K6, and MBOP9-K14, respectively. The dimensions of the upper-level decision variables n_{u} of MBOP13 to MBOP15 are set to be 5, 4, 4.

The parameter settings of Classic1 and Classic2 could be found in the last line but two and the last line but one of Table V, and the other parameter settings of the classical methods are the same as those in the original paper. Moreover, the parameter setting of the practical problem is given in the last line of Table V.

II. Appendix B

This section verifies the effectiveness of TKDEA. First, the effectiveness of the TKDEA is investigated on the MBOP. Next, we compare the proposed algorithm with some classical methods. In addition, to verify the performance of TKDEA on practical problem, we compare it on a petroleum refining problem. Then, to verify the validity of our proposed algorithm, we use an ablation study for comparison. Finally, sensitivity study is performed to analyze the effects of the parameter and hyperparameters.

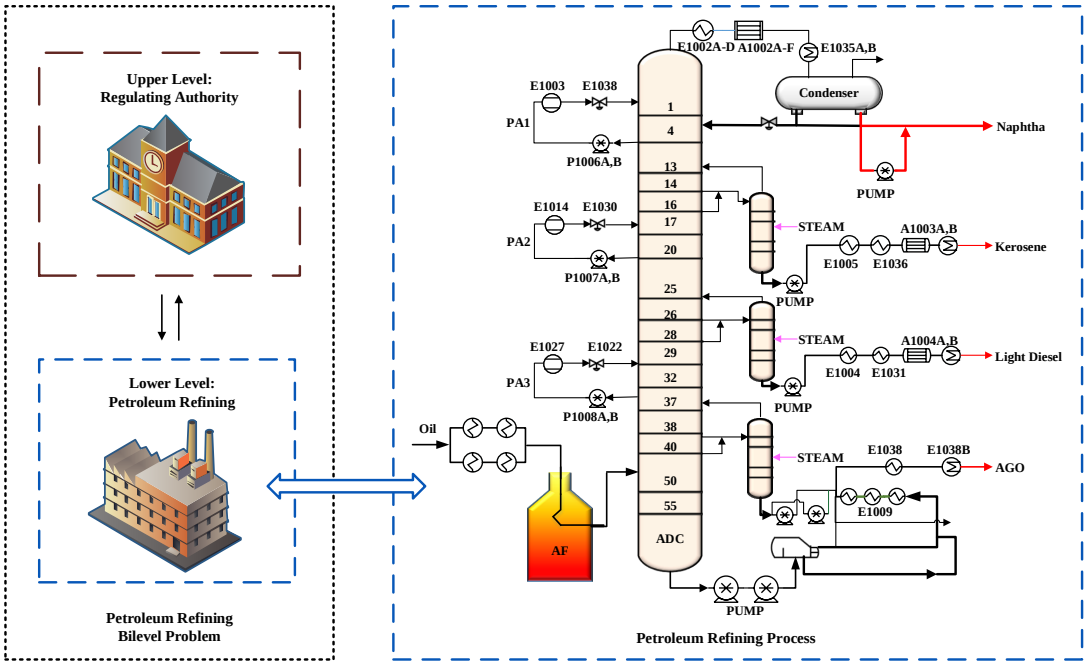

Fig. 1. The illustrative diagram of the structure of the practical petroleum refining MBLOP.

A. Comparisons with the peer algorithms

The statistical comparison results of IGD, HV, and IGD+ values, based on the Wilcoxon signed-rank test, are given in Table VI. From these results, we can see that TKDEA obtains the better results. In the following paragraph, we analyze the performance instance by instance.

MBOP1 to MBOP7 are test problems characterized by multi-modalities and scalable. TKDEA has achieved the best results on almost all the test problems. As for MBOP8, BLEMO obtains better IGD and HV values while TKDEA obtains a better IGD+ value. Indeed, only some critical solutions at the lower level will respond to the optimal solution of the upper level. TKDEA may not find these solutions, resulting in the performance of TKDEA is not promising. MBOP9 is a difficult test problem. If the algorithm fails to find the lower-level Pareto-optimal set, these infeasible solutions are likely to dominate the true Pareto-optimal solutions at the upper level. For the MBOP9 on different lower-level variable dimensions, TKDEA is very competitive among all the dimensions and significantly better performance than the others. In terms of MBOP10, our proposed algorithm obtains the second-best performance. MBOP11 is a practical problem that lacks real PF, and we can see that TKDEA is significantly better than the other two algorithms.

Moreover, to have a better visual presentation of the solutions, the non-dominated solutions obtained by the three algorithms are presented in Fig. 2 and Fig. 3. From those plots, it is clear to see that TKDEA can converge to real PF faster with better diversity than the other selected algorithms.

Next, we analyze the numerical solution of MBOP11. MBLOP is a strongly NP-hard problem, so it is difficult to find the optimal bilevel solution. Only one numerical solution of MBOP11 is given in the original paper [13], i.e., ($\mathbf{x}^{\mathrm{U}} =$

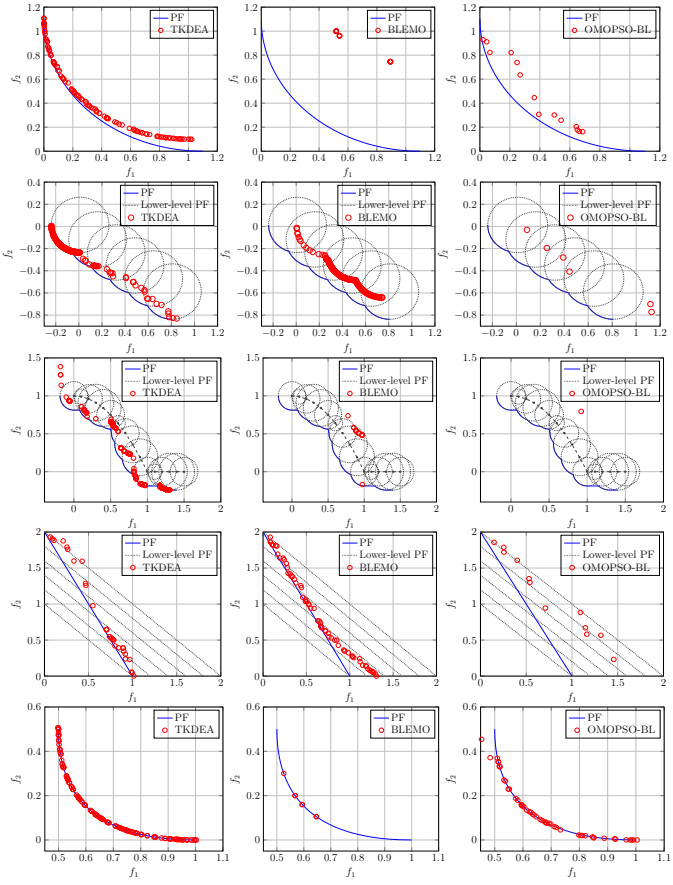

Fig. 2. Upper-level non-dominated solutions obtained by three MBLO algorithms on MBOP1, MBOP2, MBOP3, MBOP6, and MBOP9 test problems.

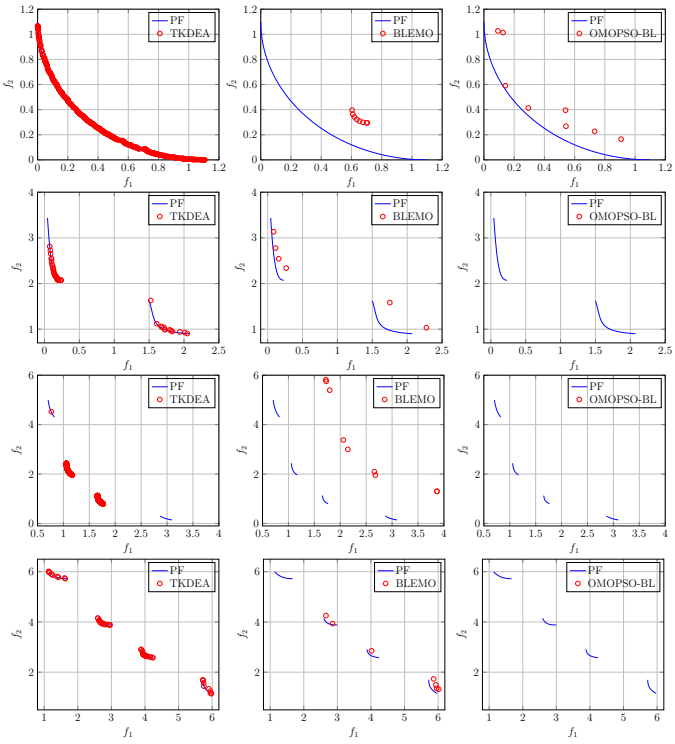

Fig. 3. Upper-level non-dominated solutions obtained by three MBLO algorithms on the test problems proposed by us (i.e., MBOP12 to MBOP15).

$(146.2955, 28.9394), \mathbf{x}^{\mathrm{L}} = (0, 67.9318, 0))$. This numerical solution provides a good guide for subsequent research. However, we notice that some nondominated solutions are not discovered in most existing papers. In this paper, we give four approximate nondominated solutions. Their variables are as follows: A: $(\mathbf{x}^{\mathrm{U}} = (0.5600, 107.5164), \mathbf{x}^{\mathrm{L}} = (0, 0, 23.2238))$, B: $(\mathbf{x}^{\mathrm{U}} = (16.6666, 100), \mathbf{x}^{\mathrm{L}} = (0, 0, 29.6665))$, C: $(\mathbf{x}^{\mathrm{U}} = (92.9000, 64.4244), \mathbf{x}^{\mathrm{L}} = (0, 0, 60.1598))$, and D: $(\mathbf{x}^{\mathrm{U}} = (146.1023, 29.0719), \mathbf{x}^{\mathrm{L}} = (0, 67.6585, 0.2501))$. $\mathbf{x}^{\mathrm{L}}$ is the approximate optimal lower-level decision variable we could find in the case of a fixed upper-level decision variable. It's worth noting that these solutions may not be the true bilevel optimal solutions (due to the strongly NP-hard of MBLOP), but these solutions are not dominated by the solutions obtained in the existing paper. The overall upper-level nondominated solutions obtained by TKDEA are shown in Fig. 4, which shows TKDEA could find a set of good performance solutions. The corresponding upper- and lower-level objective vectors could be found in Table VII.

MBOP12 to MBOP15 are test problems that contain scalable, deceptive, continuous, and discontinuous properties. And we can clearly see that TKDEA has much better performance than the comparison algorithms in terms of IGD, HV, and IGD+, demonstrating its effectiveness in tackling these test problems.

Moreover, Table VIII shows the comparisons of the overall, upper-level, and lower-level function evaluations (dubbed FE, ULFE, LLFE) achieved by three multiobjective bilevel optimization algorithms. The distribution and variance of IGD, HV and, IGD+ are given in Fig. 5, Fig. 6 and Fig. 7, respectively.

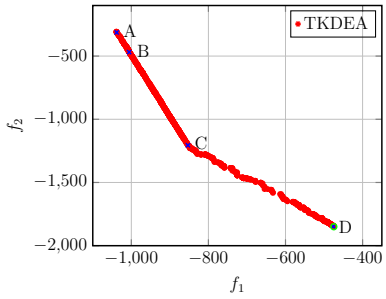

Fig. 4. Upper-level non-dominated solutions obtained by TKDEA on MBOP11. The point marked with a circle is taken from [13].

Note that the IGD+ values of MBOP10 and MBOP11 are not available due to the lack of their real PFs. It can be seen from the above results that TKDEA achieves better performance than the other two algorithms.

B. Comparisons with classical methods

Due to Classic1 and Classic2 lacking real PFs, we only calculate the HV values. Table IX and Table X give the detailed HV values of the compared algorithms. As can be seen from these results, TKDEA has an obvious advantage over CA1 and CA2 on Classic1 and obtains a better HV value on Classic2 than CA3. Moreover, the obtained approximate PF is given in Fig. 8. As can be seen from these results, TKDEA has an obvious advantage over CA1 and CA2 on Classic1 and obtains a better HV value on Classic2 than CA3. In addition, Fig. 8 shows that the solutions obtained by TKDEA are more uniform than those obtained by these classical methods.

C. Comparison Results on a Petroleum Refining Problem

The overall flow chart of the practical petroleum refining MBLOP is given in Fig. 1. The regulating authority plays a leading role and aims to earn revenues through taxes and regulate the environmental damages. On the other hand, the petroleum refining enterprise reacts rationally to the decisions of the leader to maximize its profit and minimize its burnt fuel. The limited non-renewable crude oil resources and rising prices of burnt fuel are forcing the enterprises to achieve their objectives via operational optimization.

Based on the comparison results in Table XI, we can see that TKDEA achieved the best HV value compared to the other peers. As the plots of the non-dominated solutions obtained by three peer algorithms shown in Fig. 9, the solutions obtained by TKDEA explicitly dominate the others. In particular, the solutions obtained by OMOPSO-BL are randomly scattered in the objective space and are mostly dominated by TKDEA and BLEMO. Besides, as shown in Table XI, we can see that TKDEA and BLEMO consume the same number of function evaluations. In contrast, it is also worth noting that OMOPSO-BL consumes $109,680$ more function evaluations than TKDEA and BLEMO, but it still fails to find meaningful solutions as shown in Fig. 9.

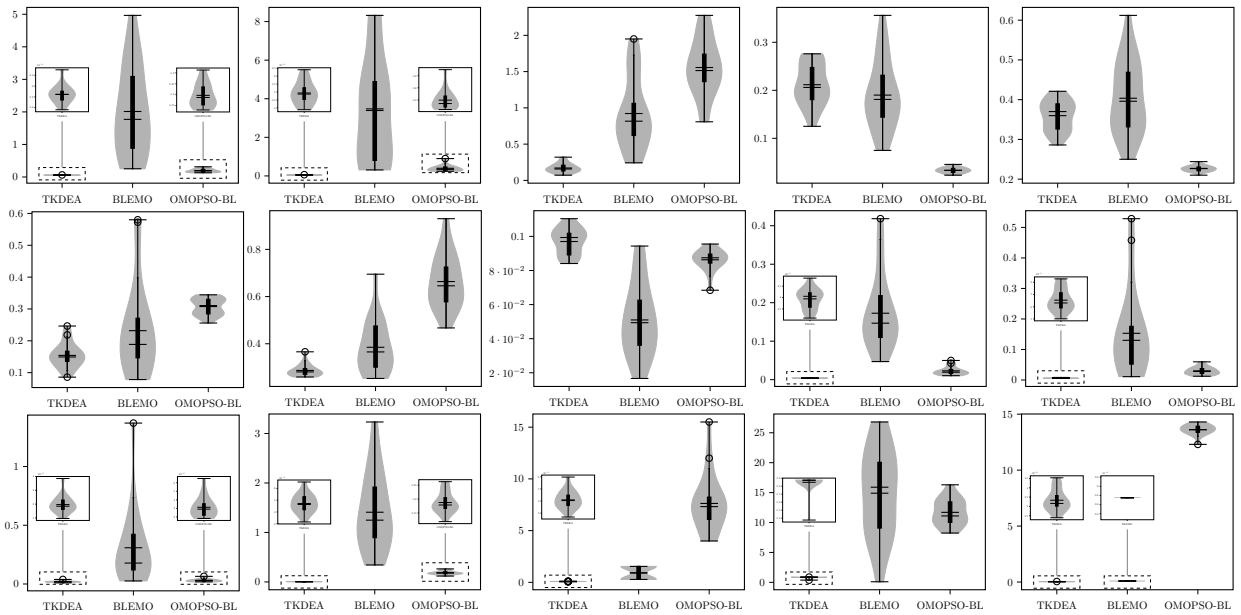

Fig. 5. Violin plots and box plots of IGD achieved by three multiobjective bilevel optimization algorithms (The part corresponding to the dashed line is the enlarged plot).

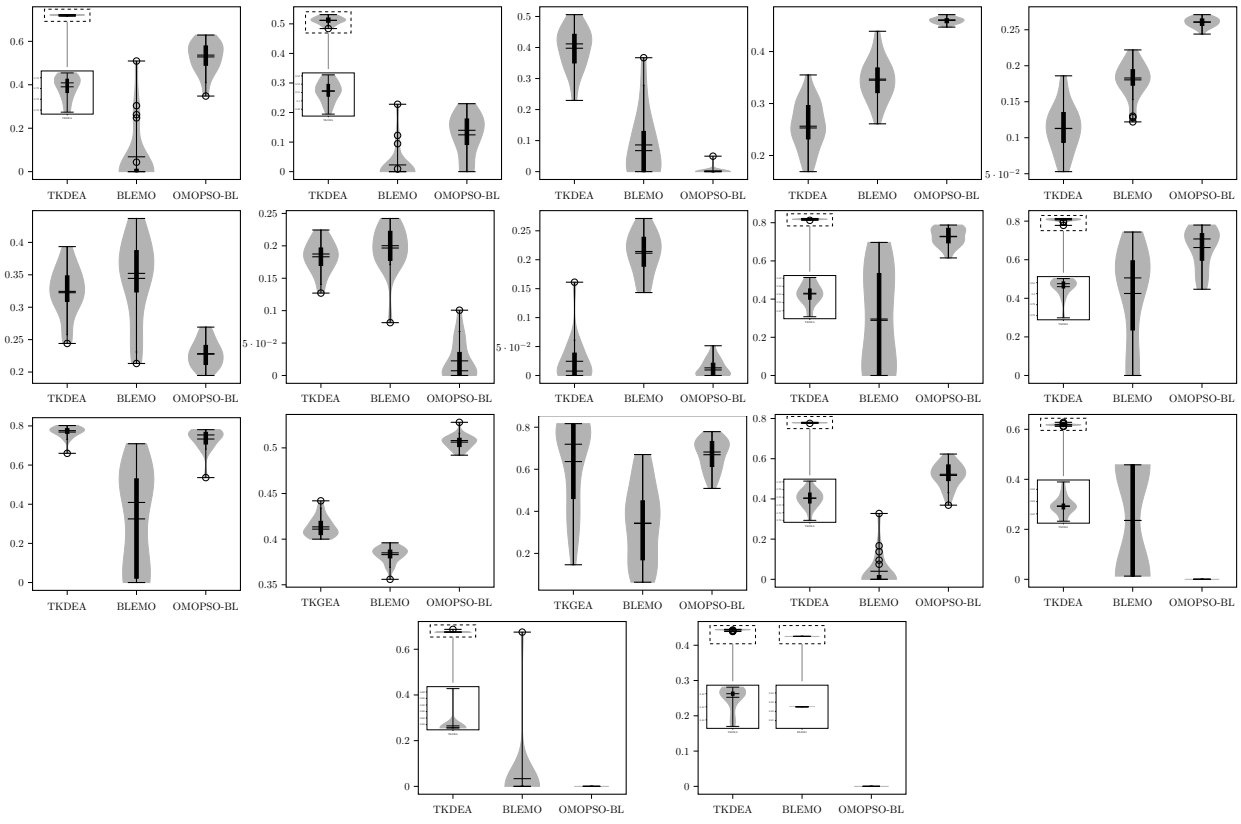

Fig. 6. Violin plots and box plots of HV achieved by three multiobjective bilevel optimization algorithms (The part corresponding to the dashed line is the enlarged plot).

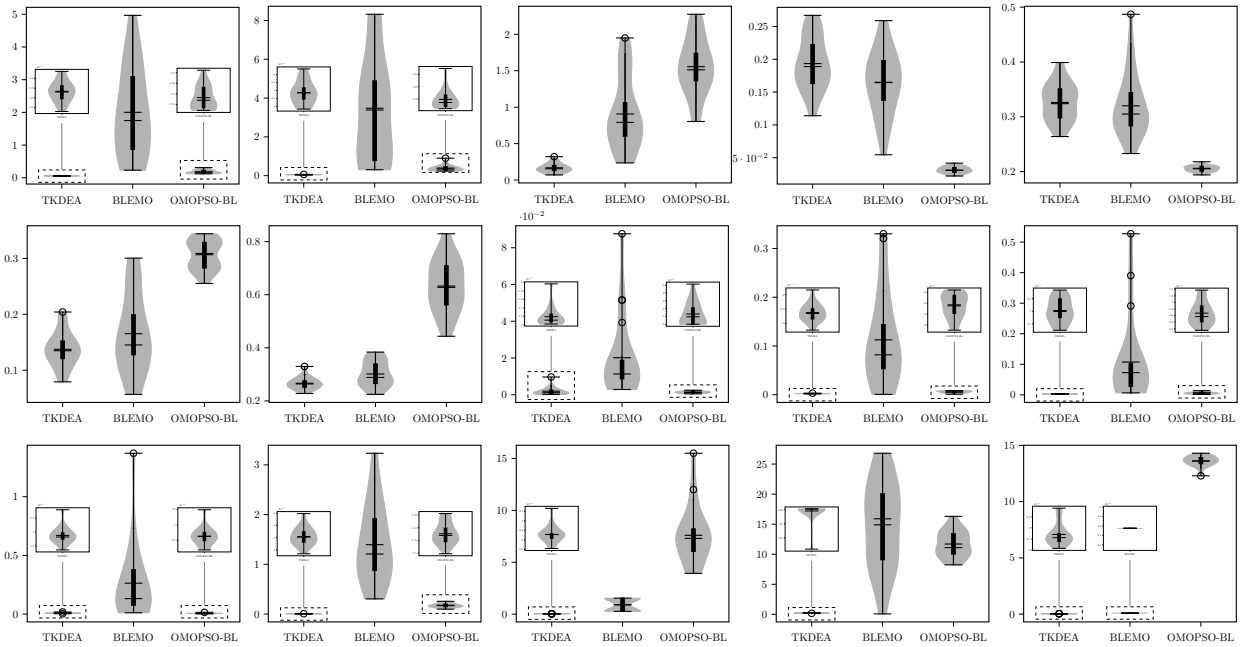

Fig. 7. Violin plots and box plots of IGD+ achieved by three multiobjective bilevel optimization algorithms (The part corresponding to the dashed line is the enlarged plot).

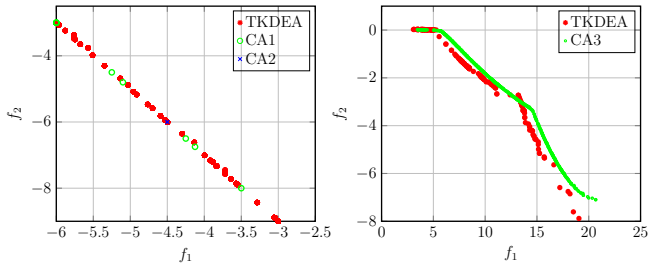

Fig. 8. Upper-level non-dominated solutions obtained by TKDEA, CA1, and CA2 on Classic1 (left). Upper-level non-dominated solutions obtained by TKDEA and CA3 (right).

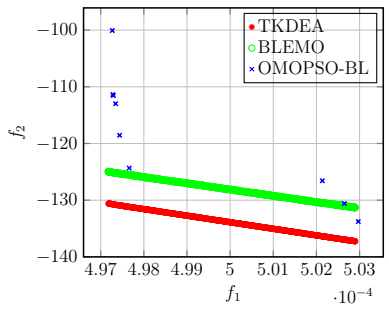

Fig. 9. Upper-level non-dominated solutions obtained by TKDEA, BLEMO, and OMOPSO-BL on the petroleum refining problem.

D. Ablation Study

To validate the competitiveness of the proposed lower-level algorithm, we use ablation study to investigate the effect of the lower-level algorithm.

1) Effectiveness of the lower-level algorithm: We first use ablation study to compare the proposed lower-level algorithm with several single-level constrained multiobjective algorithms (i.e., TKDEA, C-TAEA, I-DBEA, and DMOEA-εC). The codes for C-TAEA, I-DBEA, and DMOEA-εC are available on the PlatEMO [14]. All the algorithms are combined with the multiobjective bilevel optimization solving procedure introduced in Section III-D. The corresponding multiobjective bilevel algorithms are dubbed B-x, where x is either C-TAEA, I-DBEA, or DMOEA-εC. Under the same solving procedure and generation settings, the number of function evaluations of the rest algorithms is the same as TKDEA. The statistical comparison results of IGD, IGD+, and HV values, based on the Wilcoxon signed-rank test, are presented in Table XII.

From these results, we can see that TKDEA significantly outperforms the other algorithms on most of the test problems. Especially in MBOP9 of different lower-level decision variable dimensions, TKDEA shows a competitive performance compared with other algorithms. For MBOP2, B-DMOEA-εC achieves the best performance, while TKDEA does not perform very well. The reason may be that the upper-level population on MBOP2 test problem is easier trapped in local optimum due to the multi-modality of upper-level optimization problem. Thus causing TKDEA to fall into local optimum. According to the Wilcoxon signed-rank test, TKDEA obtains the best results on 51 and similar results on 29 out of 105 test problems. Moreover, the A_{12} effect size of four algorithms is given in Fig. 10. According to the A_{12} effect size of four algorithms, and the large effect sizes are 37%, 49%, and 54%, respectively. Moreover, we apply the Scott-Knott test to sort the performance of four algorithms. The Scott-Knott result is presented in Fig. 11. And we can clearly see from the result that TKDEA obtains first rank. After that, to observe the results intuitively, the data distributions of the IGD, HV, and IGD+ are given as violin plots and box plots in Fig. 12, Fig. 13, and Fig. 14, respectively. From these results, we can clearly

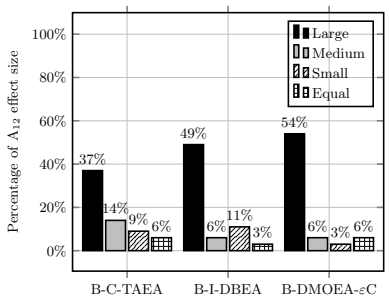

Fig. 10. Percentage of A_{12} effect size of three single-level algorithms combined with the same upper-level solving procedure compared with TKDEA.

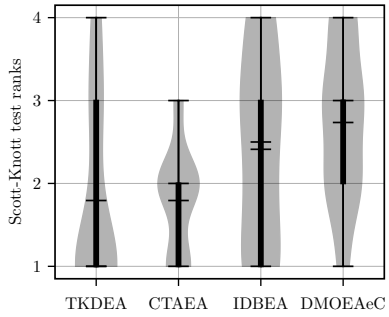

Fig. 11. Violin plots and box plots of Scott-Knott test ranks achieved by four algorithms (the smaller rank is, the better performance achieved).

see that our proposed algorithm has more centralized data distributions and obtains better results. Thus, we can conclude that TKDEA is competitive in dealing with the MBLOP.

2) Effectiveness of two stages: The above empirical study has shown that the proposed lower-level algorithm has better performance than the selected constrained multiobjective algorithms. The lower-level algorithm of TKDEA is composed of two stages. We empirically investigate the performance of TKDEA w.r.t. the variant TKDEA−S1 only uses the `first-stage search` step, and the variant TKDEA−S2 only uses the `second-stage search` step.

From the statistical comparison results of IGD, HV, and IGD+ results, A_{12} effect size results are shown in Fig. 15. We have witnessed a performance degradation when ablating any of the stages. And the sum of the better A_{12} effect size is 63% for TKDEA−S1 and 74% for TKDEA−S2. In addition, to facilitate an overall comparison, we further apply the Scott-Knott test to sort the performance of the compared algorithms, which is given in Fig. 16. TKDEA has shown the best performance, TKDEA−S1, TKDEA−S2, OMOPSO−BL, and BLEMO obtain second, third, fourth, and fifth ranks. Moreover, the upper-level nondominated solutions of three algorithms on MBOP9-K14 is given in Fig. 17. From the figure, we can see that TKDEA can obtain more uniform solutions than TKDEA−S1 and TKDEA−S2. From these results, we further confirm that TKDEA is better than TKDEA−S1 and TKDEA−S2 in the corresponding comparison.

E. Parameter Sensitivity Study

In our proposed algorithm, there is a switching parameter α in the lower-level algorithm. To study the impact of parameter, we choose TKDEA as the baseline and empirically investigate the performance under different $\alpha = \{0.1, 0.3, 0.5, 0.7, 0.9\}$ settings. Fig. 18, Fig. 19, and Fig. 20 give the box plots of IGD, HV, and IGD+ on MBOP1 to MBOP8 and MBOP9(with different lower-level decision variable dimensions, $K = 2, 6, 14$). From these figures, we can see that different α results in different performances. In this paper, we set the parameter α to 0.3.

F. Hyperparameter Sensitivity Study

In what follows, we consider the sensitivity of different hyperparameters on the convergence of the algorithm. We select TKDEA as our baseline and conduct empirical experiments to assess its performance across various sets of hyperparameters on MBOP1 to MBOP9. The experiment examines six hyperparameters: the probability of crossover p_c, the probability of mutation p_m, the upper-level population size N^{U}, the lower-level population size N^{L}, the upper-level iteration T^{U}, and the lower-level iteration T^{L}. Furthermore, we used three performance metrics, IGD, HV, and IGD+, to assess the convergence performance. To thoroughly assess the impact of hyperparameters on convergence, we configured five different parameter values for these hyperparameters except T^{U}. Specifically, the hyperparameters are $p_c = \{0.6, 0.7, 0.8, 0.9, 1\}$, T^{U} changes in intervals of 10 from 0 to 500, and the remaining hyperparameters are listed in Table XIII. We vary the value of a particular hyperparameter while keeping the other hyperparameters constant to assess the impact of the current hyperparameter on the algorithm.

With increasing upper-level generation, the IGD, HV, and IGD+ of different p_c values are shown in Fig. 21, Fig. 22, and Fig. 23. We can see that, at the beginning of the evolution, TKDEA exhibits a faster convergence performance on most test problems when employing a larger crossover probability. A larger crossover probability may facilitate better information sharing, thereby effectively exploring the potential solution space. However, in the subsequent evolution, the various p_c values do not yield notably distinct effects. Especially on MBOP1, MBOP2, and MBOP9, TKDEA with varying p_c values shows nearly consistent change trends. This may be due to the algorithm having a sufficient number of function evaluations to approximate the PF.

In the following, Fig. 24, Fig. 25, and Fig. 26 illustrate the performance of p_m with increasing upper-level generations. From these figures, we can see that the effect of p_m on these test problems is problem-specific, with no consistent pattern. In most cases, the convergence performance is not very sensitive to p_m. This may be due to the complexity of the problem itself, and as a result, the convergence performance is not greatly affected by this hyperparameter.

In addition, the changes in performance metrics of different N^{U} are shown in Fig. 27 to Fig. 29 ; those for various N^{L} are shown in Fig. 30 to Fig. 32. Compared with p_m and p_c, N^{U} shows a greater effect on convergence. As shown in Fig. 27 to Fig. 29, the algorithm converges faster when N^{U} is larger. This is because a larger upper-level population can accommodate more solutions with good performance.

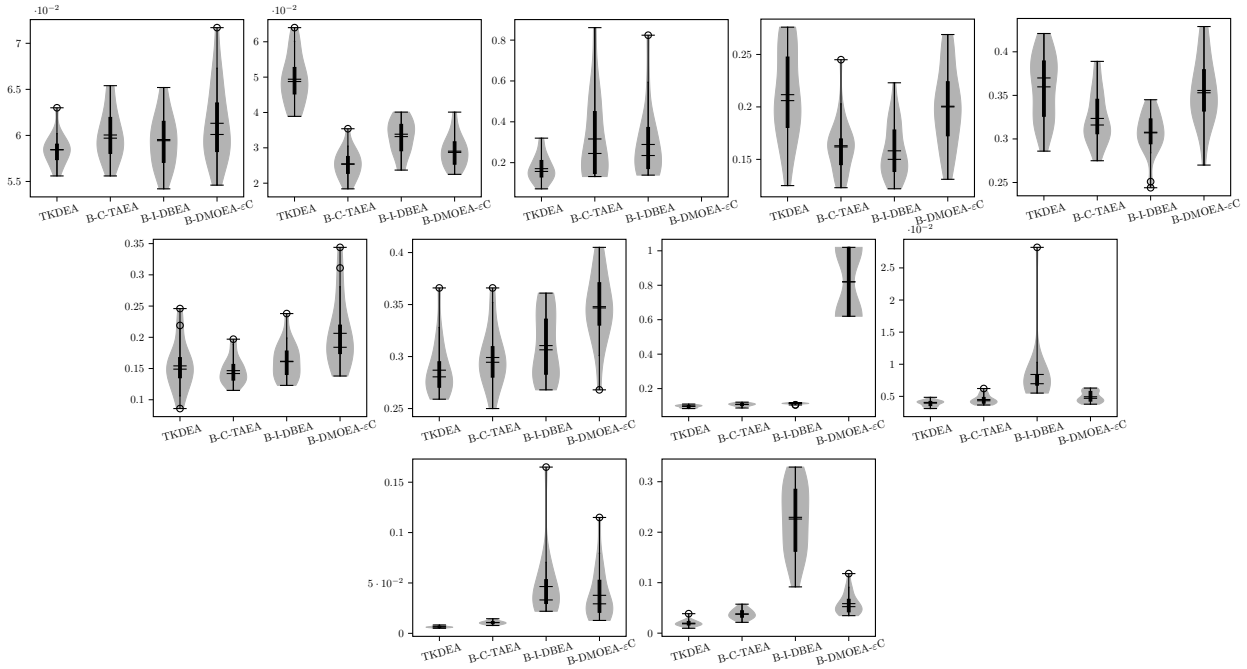

Fig. 12. Violin plots and box plots of IGD achieved by four algorithms (The part corresponding to the dashed line is the enlarged plot).

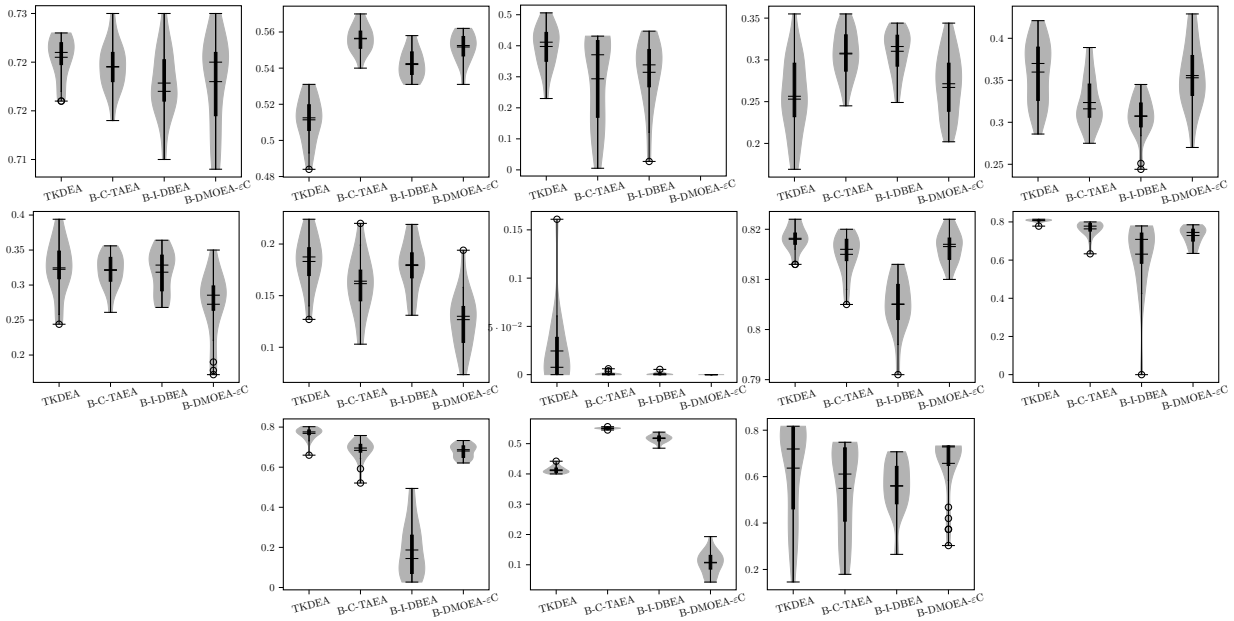

Fig. 13. Violin plots and box plots of HV achieved by four algorithms(The part corresponding to the dashed line is the enlarged plot).

Clearly, N^{U} impacts the balance between exploration and exploitation, but it is a double-edged sword. A small upper-level population consumes fewer function evaluations, but the algorithm is easily trapped in local optima. On the flip side, a larger upper-level population provides more exploration opportunities and converges faster, but it also comes with increased computational costs.

Regarding the impact of hyperparameter N^{L} on convergence, N^{L} also affects the balance between exploration and exploitation. Based on the results from Fig. 30 to Fig. 32, we can see that the convergence of algorithm with smaller N^{L} is worse than those with larger N^{L} in most cases. This may be because a smaller lower-level population may limit exploration opportunities, leading the algorithm to get trapped in local optima. A larger lower-level population, on the other hand, can handle more solutions simultaneously, which helps explore the solution space effectively and accelerates the convergence speed of the algorithm.

Next, Fig. 33 to Fig. 35 and Fig. 36 to Fig. 38 depict the changes of IGD, HV, and IGD+ under different upper- and lower-level iterations, respectively. As expected, increasing T^{U} typically leads to improved algorithm convergence in

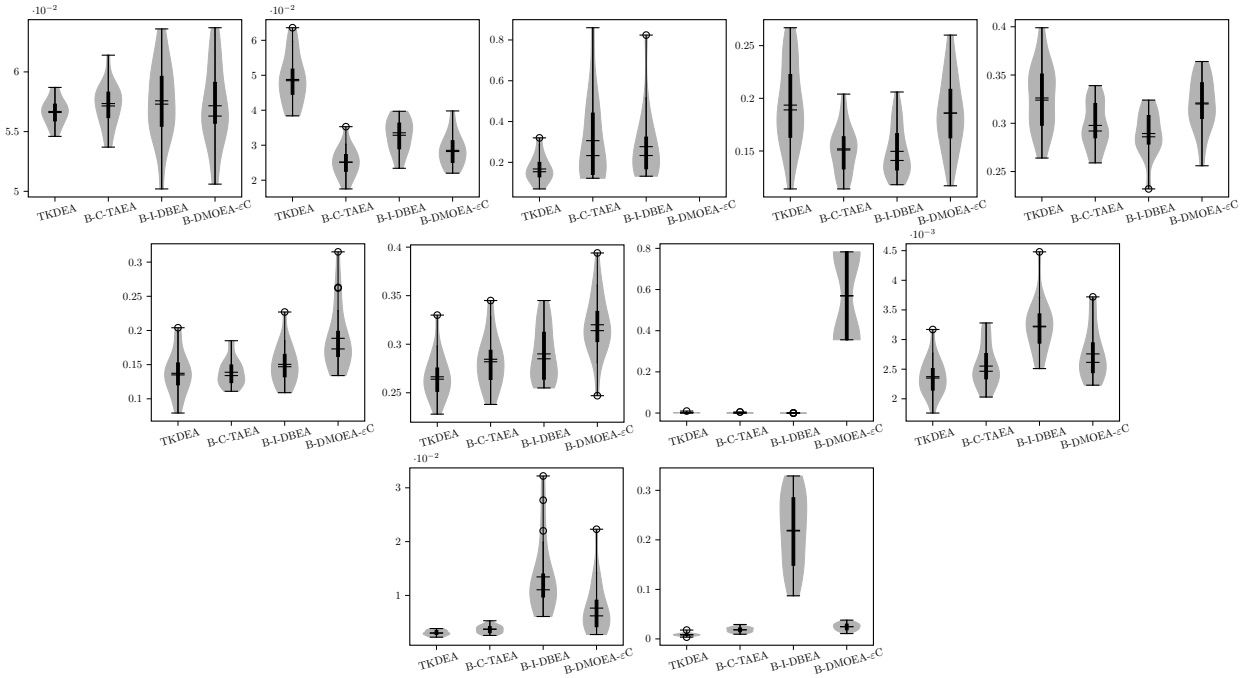

Fig. 14. Violin plots and box plots of IGD+ achieved by four algorithms (The part corresponding to the dashed line is the enlarged plot).

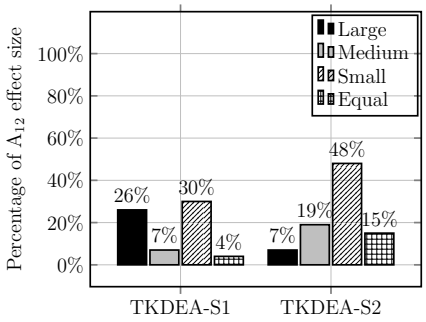

Fig. 15. Percentage of A_{12} effect size of two algorithms.

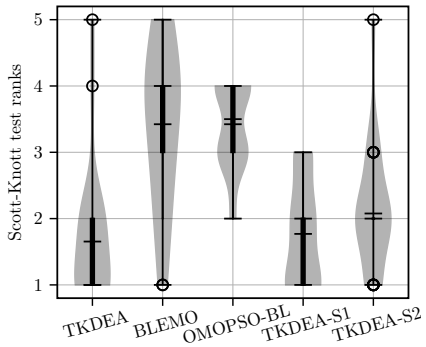

Fig. 16. Violin plots and box plots of Scott-Knott test ranks achieved by five algorithms (the smaller rank is, the better performance achieved).

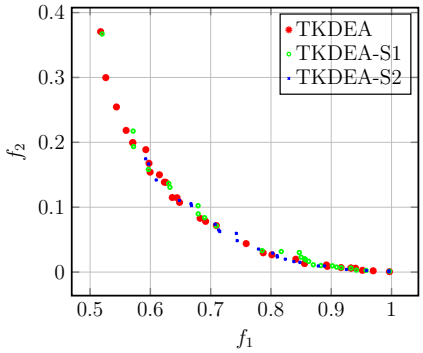

Fig. 17. Two stages of effectiveness on MBOP11-K14

most cases (e.g., from MBOP1 to MBOP8). As T^{U} increases, more solutions could be evaluated. However, this trend is not applicable to deceptive problems. In deceptive problems, if the lower-level problem is not solved precisely, constantly increasing T^{U} may have the opposite effect, where deceptive solutions dominate the true Pareto optimal solutions. In such cases, it is more effective to increase T^{L} rather than increasing T^{U} to improve convergence.

Finally, we conducted experiments to analyze the effect of T^{L} on convergence. If the other hyperparameters remain consistent, in most cases, increasing T^{L} leads to better convergence. When T^{L} is small, `TKDEA` struggles to converge quickly in certain upper-level function evaluations. However, if T^{L} is too large, although the algorithm obtains precise solutions, it comes at the cost of consuming a significant number of function evaluations. Based on the experimental results, we can conclude that `TKDEA` exhibits good convergence performance under the T^{L} we set, and the hyperparameter settings are reasonable.

REFERENCES

[1] K. Deb, L. Thiele, M. Laumanns, and E. Zitzler, "Scalable test problems for evolutionary multiobjective optimization," in *Evolutionary Multiobjective Optimization*, ser. Advanced Information and Knowledge Processing, A. Abraham, L. C. Jain, and R. R. Goldberg, Eds. Springer, 2005, pp. 105–145.

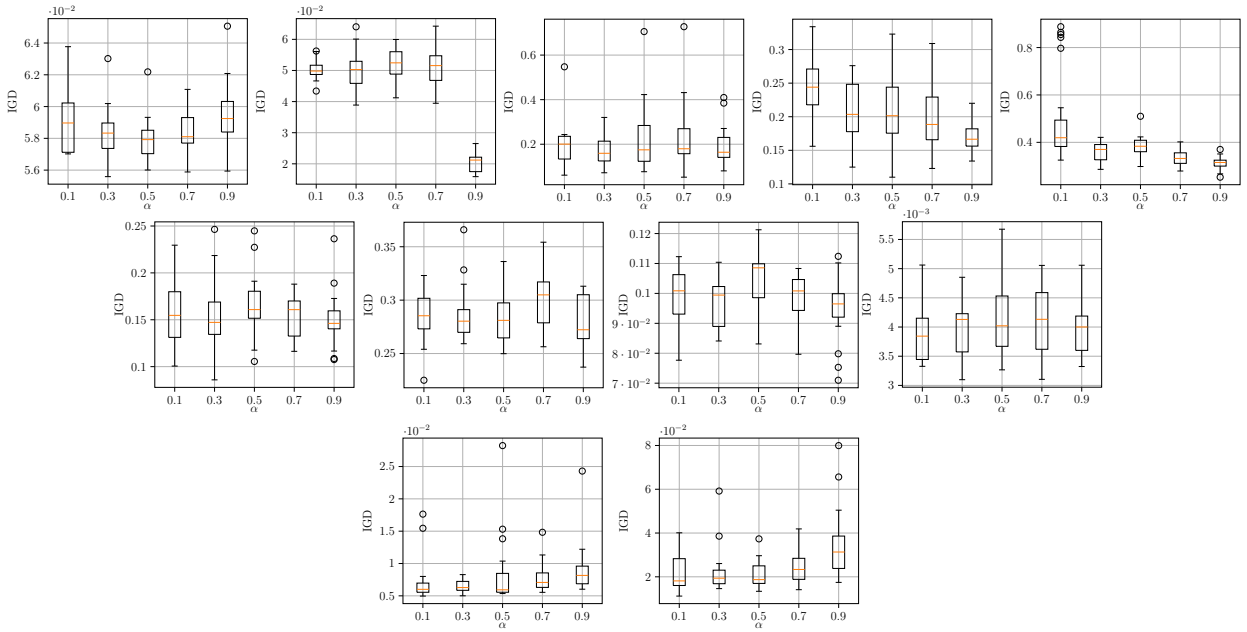

Fig. 18. Collected comparisons of IGD when using different α settings.

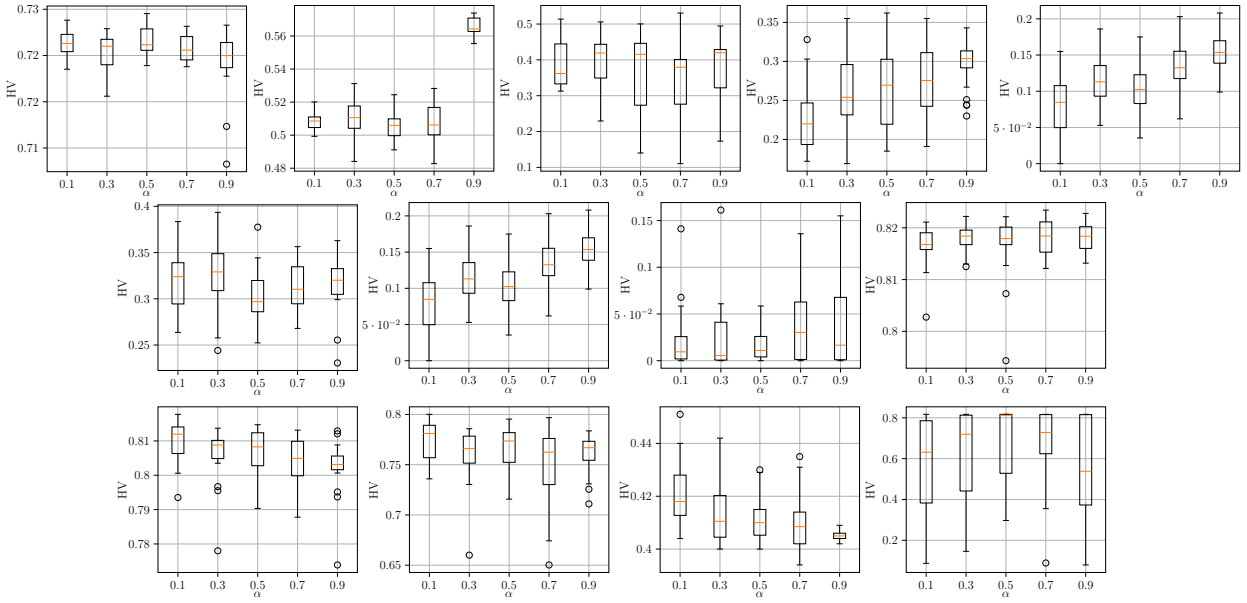

Fig. 19. Collected comparisons of HV when using different α settings.

[2] K. Deb and A. Sinha, "An efficient and accurate solution methodology for bilevel multi-objective programming problems using a hybrid evolutionary-local-search algorithm," *Evol. Comput.*, vol. 18, no. 3, pp. 403–449, 2010.

[3] J. Branke, K. Deb, H. Dierolf, and M. Osswald, "Finding knees in multi-objective optimization," in *PPSN'04: Proc. of the 8th International Conference on Parallel Problem Solving from Nature*, ser. Lecture Notes in Computer Science, vol. 3242. Springer, 2004, pp. 722–731.

[4] L. Rachmawati and D. Srinivasan, "Multiobjective evolutionary algorithm with controllable focus on the knees of the pareto front," *IEEE Trans. Evol. Comput.*, vol. 13, no. 4, pp. 810–824, 2009.

[5] C. O. Pieume, P. Marcotte, L. P. Fotso, and P. Siarry, "Solving bilevel linear multiobjective programming problems," *Am. J. Oper. Res.*, vol. 1, no. 4, pp. 214–219, 2011.

[6] M. H. Farahi and E. Ansari, "A new approach to solve multi-objective linear bilevel programming problems," *J. Math. Comput. Sci.*, vol. 1, no. 4, pp. 313–320, 2010.

[7] G. Eichfelder, "Multiobjective bilevel optimization," *Mathematical Programming*, vol. 123, no. 2, pp. 419–449, 2010.

[8] ——, *Solving nonlinear multiobjective bilevel optimization problems with coupled upper level constraints*, 2007.

[9] Y. Chen, J. Ding, and T. Chai, "A knowledge transfer based scheduling algorithm for large-scale refinery production," *IEEE Trans. Ind. Informatics*, vol. 18, no. 2, pp. 869–879, 2022.

[10] Q. Chen, J. Ding, T. Chai, and Q. Pan, "Evolutionary optimization under uncertainty: The strategies to handle varied constraints for fluid catalytic cracking operation," *IEEE Trans. Cybern.*, vol. 52, no. 4, pp. 2249–2262, 2022.

[11] J. Lu, J. Ding, C. Liu, and T. Chai, "Hierarchical-bayesian-based sparse stochastic configuration networks for construction of prediction intervals," *IEEE Trans. Neural Networks Learn. Syst.*, pp. 1–12, 2021.

[12] M. Gadalla, Ž. Olujić, M. Jobson, and R. Smith, "Estimation and reduction of co2 emissions from crude oil distillation units," *Energy*, vol. 31, no. 13, pp. 2398–2408, 2006.

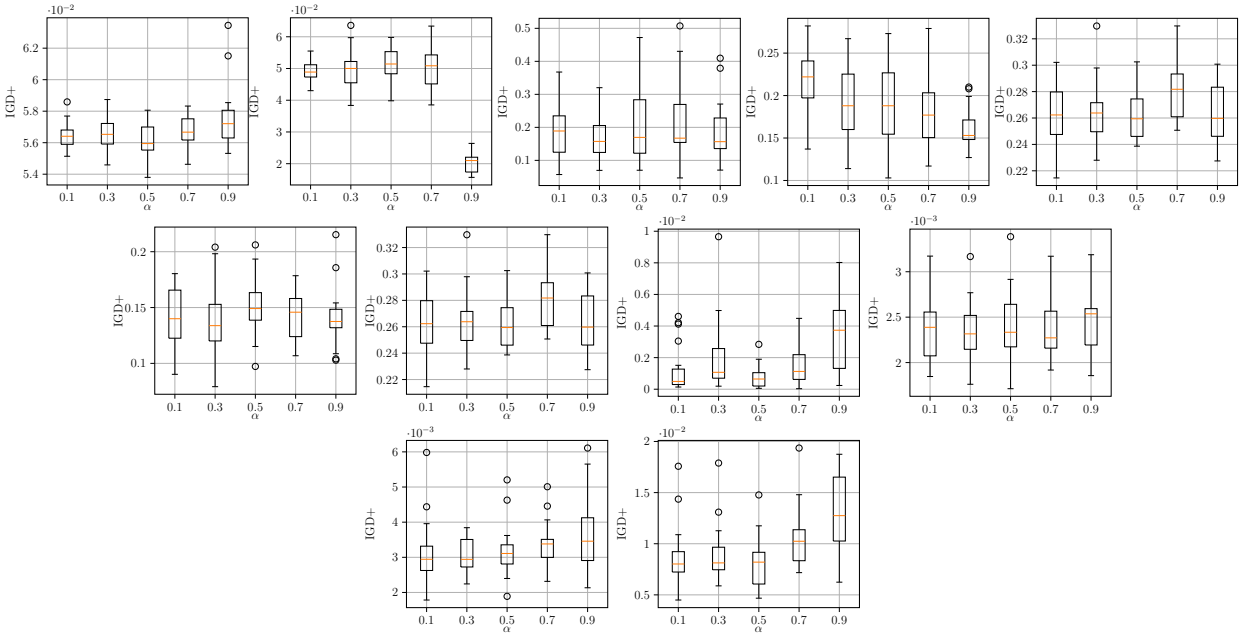

Fig. 20. Collected comparisons of IGD+ when using different α settings.

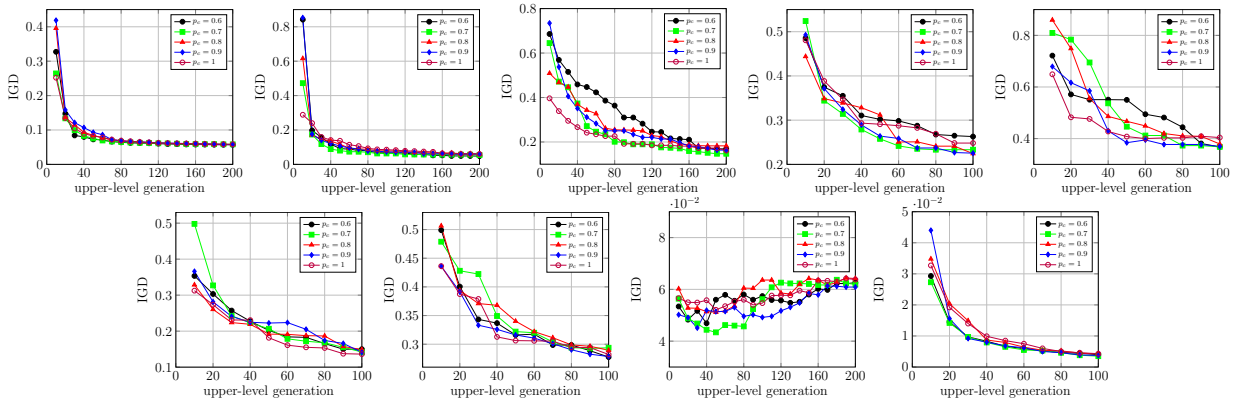

Fig. 21. Influence of the hyperparameter p_c on the convergence measuring by IGD.

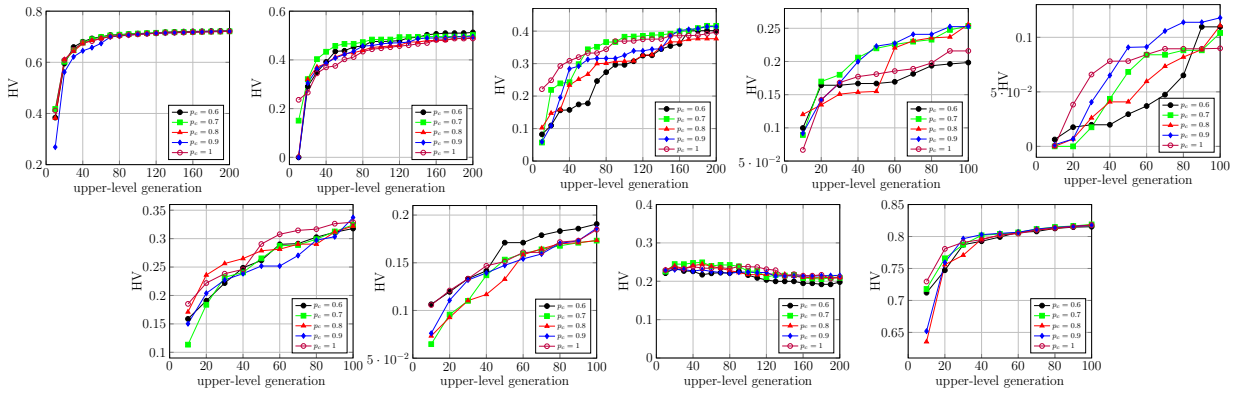

Fig. 22. Influence of the hyperparameter p_c on the convergence measuring by HV.

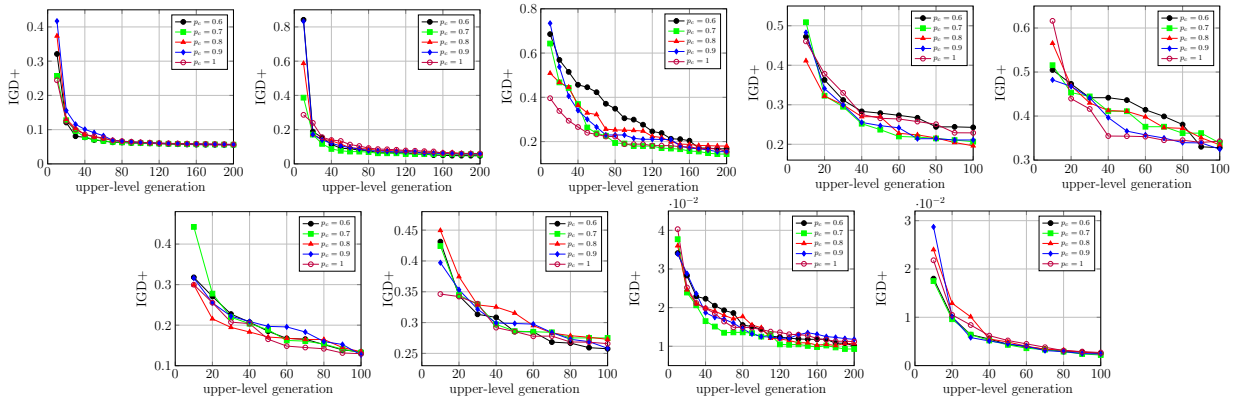

Fig. 23. Influence of the hyperparameter p_c on the convergence measuring by IGD+.

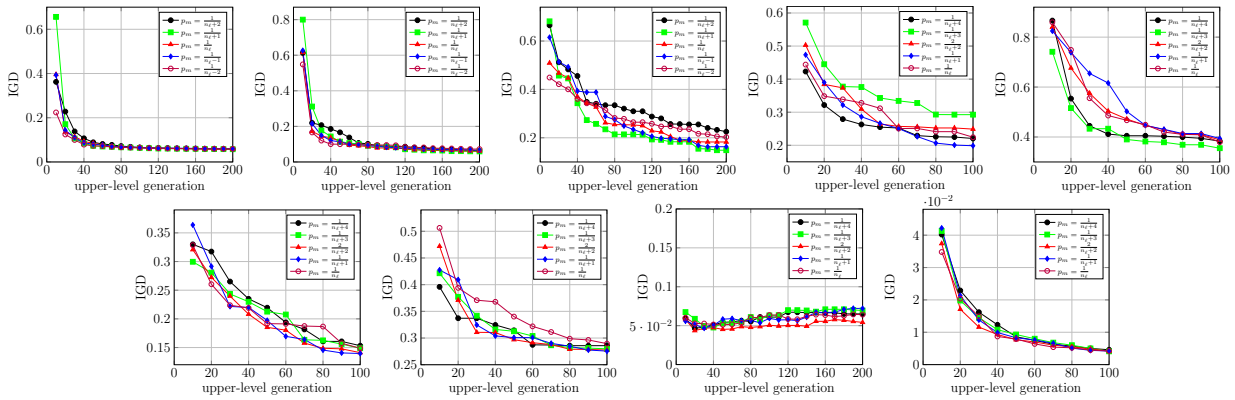

Fig. 24. Influence of the hyperparameter p_m on the convergence measuring by IGD.

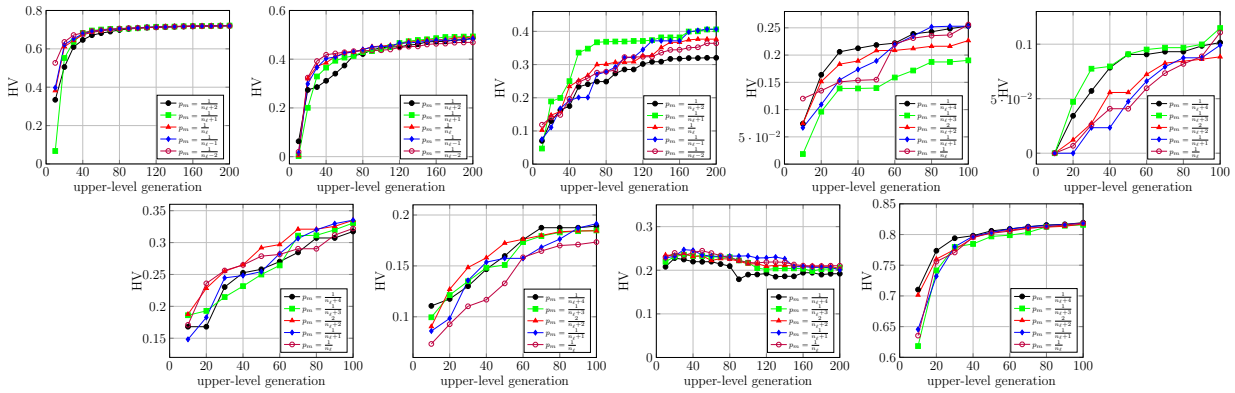

Fig. 25. Influence of the hyperparameter p_m on the convergence measuring by HV.

[13] G. Zhang, J. Lu, and T. S. Dillon, "Decentralized multi-objective bilevel decision making with fuzzy demands," *Knowl. Based Syst.*, vol. 20, no. 5, pp. 495–507, 2007.

[14] Y. Tian, R. Cheng, X. Zhang, and Y. Jin, "Platemo: A MATLAB platform for evolutionary multi-objective optimization," *IEEE Comput. Intell. Mag.*, vol. 12, no. 4, pp. 73–87, 2017.

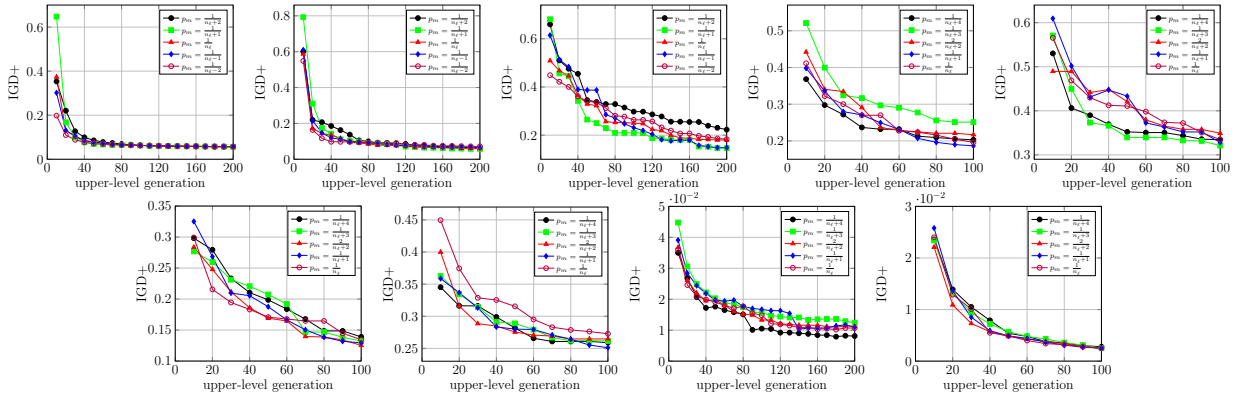

Fig. 26. Influence of the hyperparameter p_m on the convergence measuring by IGD+.

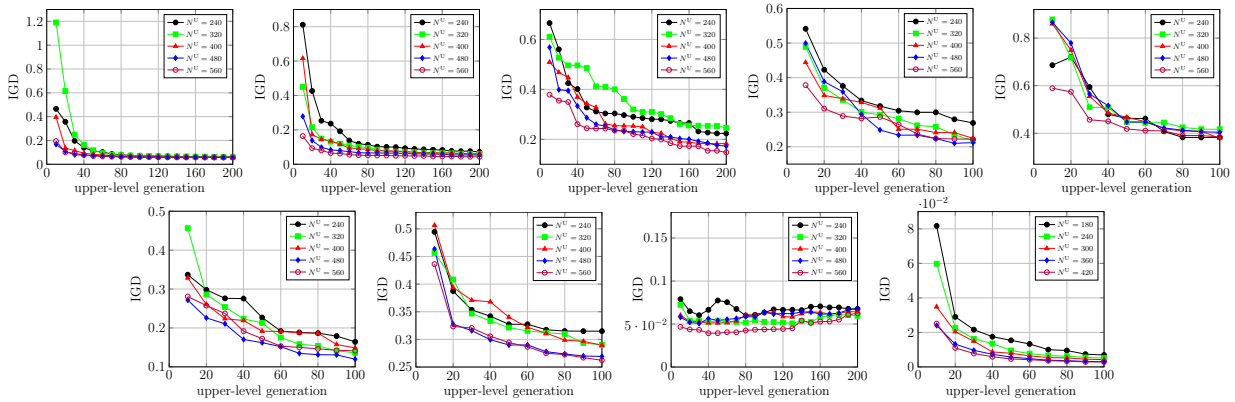

Fig. 27. Influence of the hyperparameter N^{U} on the convergence measuring by IGD.

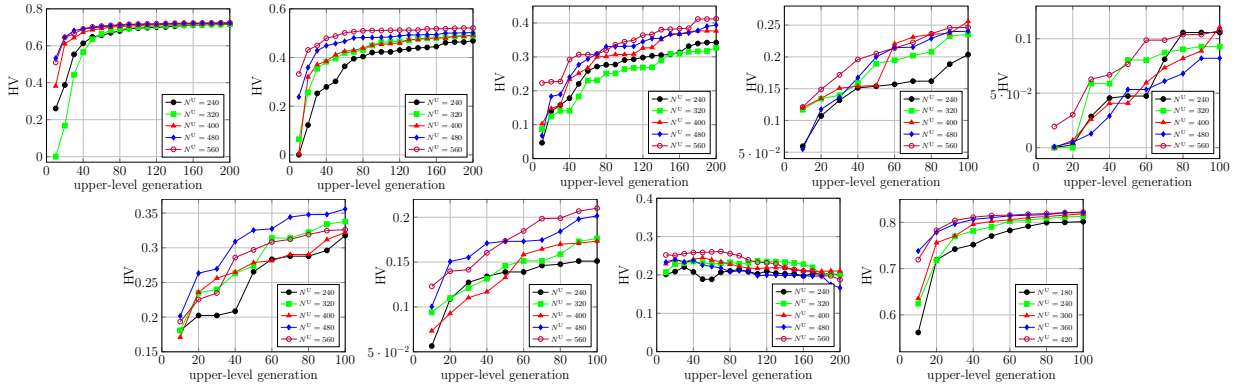

Fig. 28. Influence of the hyperparameter N^{U} on the convergence measuring by HV.

TABLE I
PROPOSED TEST PROBLEM

Test problem	Function
MBOP12	$\min\limits_{\mathbf{x}^{\mathrm{U}}\in\Omega^{\mathrm{U}},\mathbf{x}^{\mathrm{L}}\in\Omega^{\mathrm{L}}} \mathbf{F}(\mathbf{x}^{\mathrm{U}},\mathbf{x}^{\mathrm{L}}) = \begin{pmatrix} f_1(\mathbf{x}) = (1+r-\cos(\alpha\pi x_1^{\mathrm{U}})) + \sum_{j=2}^{K}(x_j^{\mathrm{U}} - \frac{j-1}{2})^2 + \tau\sum_{i=2}^{K}(x_i^{\mathrm{L}} - x_i^{\mathrm{U}})^2 - \\ r\cos\left(\gamma\frac{\pi}{2}\frac{q(x_1^{\mathrm{L}})\sin\frac{\pi x_1^{\mathrm{L}}}{2} - q(x_1^{\mathrm{L}})\cos\frac{\pi x_1^{\mathrm{L}}}{2}}{x_1^{\mathrm{U}}}\right) \\ f_2(\mathbf{x}) = (1+r-\sin(\alpha\pi x_1^{\mathrm{U}})) + \sum_{j=2}^{K}(x_j^{\mathrm{U}} - \frac{j-1}{2})^2 + \tau\sum_{i=2}^{K}(x_i^{\mathrm{L}} - x_i^{\mathrm{U}})^2 + \\ r\sin\left(\gamma\frac{\pi}{2}\frac{q(x_1^{\mathrm{L}})\sin\frac{\pi x_1^{\mathrm{L}}}{2} - q(x_1^{\mathrm{L}})\cos\frac{\pi x_1^{\mathrm{L}}}{2}}{x_1^{\mathrm{U}}}\right) \end{pmatrix}$ subject to $\mathbf{x}^{\mathrm{L}} \in \underset{\mathbf{x}^{\mathrm{L}}\in\Omega^{\mathrm{L}}}{\operatorname{argmin}} \begin{pmatrix} f_1^{\mathrm{L}}(\mathbf{x}) = q(x_1^{\mathrm{L}})\sin\frac{\pi x_1^{\mathrm{L}}}{2} + \sum_{i=2}^{K}(x_i^{\mathrm{L}} - x_i^{\mathrm{U}})^2 + \sum_{i=2}^{K} 10(1-\cos(\frac{\pi}{K}(x_i^{\mathrm{L}} - x_j^{\mathrm{U}}))) \\ f_2^{\mathrm{L}}(\mathbf{x}) = q(x_1^{\mathrm{L}})\cos\frac{\pi x_1^{\mathrm{L}}}{2} - x_1^{\mathrm{U}} + \sum_{i=2}^{K} 10\left\lvert\sin(\frac{\pi}{K}(x_i^{\mathrm{L}} - x_j^{\mathrm{U}}))\right\rvert \end{pmatrix}$ $q(x_1^{\mathrm{L}}) = 5 + 10(x_1^{\mathrm{L}} - 0.5)^2 + \frac{2^{s/2}}{\beta}\cos(2\beta\pi x_1^{\mathrm{L}})$ $1 \le x_1^{\mathrm{U}} \le 4, \quad 0 \le x_1^{\mathrm{L}} \le 1$ $K \le x_i^{\mathrm{L}}, x_i^{\mathrm{U}} \le K, \text{ for } i = 2, \cdots, K$ $r = 0.1, \alpha = 1, \tau = 1, \gamma = 1, \beta = 4, s = 0$
MBOP13	$\min\limits_{\mathbf{x}^{\mathrm{U}}\in\Omega^{\mathrm{U}},\mathbf{x}^{\mathrm{L}}\in\Omega^{\mathrm{L}}} \mathbf{F}(\mathbf{x}^{\mathrm{U}},\mathbf{x}^{\mathrm{L}}) = \begin{pmatrix} f_1(\mathbf{x}) = l(\mathbf{x}^{\mathrm{U}})r(x_1^{\mathrm{L}})\sin^3(\frac{\pi x_1^{\mathrm{L}}}{2})\big(1 + \sum_{j=2}^{K}(x_j^{\mathrm{L}})^2\big) \\ f_2(\mathbf{x}) = l(\mathbf{x}^{\mathrm{U}})r(x_1^{\mathrm{L}})\cos(\frac{\pi x_1^{\mathrm{L}}}{2})\big(1 + \sum_{j=2}^{K}(x_j^{\mathrm{L}})^2\big) \end{pmatrix}$ subject to $\mathbf{x}^{\mathrm{L}} \in \underset{\mathbf{x}^{\mathrm{L}}\in\Omega^{\mathrm{L}}}{\operatorname{argmin}} \begin{pmatrix} f_1^{\mathrm{L}}(\mathbf{x}) = l(\mathbf{x}^{\mathrm{U}})r(x_1^{\mathrm{L}})\sin^3(\frac{\pi x_1^{\mathrm{L}}}{2})\big(1 + \sum_{j=K+1}^{K+L}(x_j^{\mathrm{L}})^2\big) \\ f_2^{\mathrm{L}}(\mathbf{x}) = l(\mathbf{x}^{\mathrm{U}})r(x_1^{\mathrm{L}})\cos(\frac{\pi x_1^{\mathrm{L}}}{2})\big(1 + \sum_{j=K+1}^{K+L}(x_j^{\mathrm{L}})^2\big) \end{pmatrix}$ $l(\mathbf{x}^{\mathrm{U}}) = 1 + \frac{9}{n_{\mathrm{u}}-1}\sum_{i=1}^{n_{\mathrm{u}}} x_i^{\mathrm{U}}$ $r(x_1^{\mathrm{L}}) = 2.5 + 10(x_1^{\mathrm{L}} - 0.5)^2 + \frac{2^{s/2}}{\beta}\cos(2\beta\pi x_1^{\mathrm{L}})$ $G(\mathbf{x}^{\mathrm{U}},\mathbf{x}^{\mathrm{L}}) = f_1(\mathbf{x}) + 0.8 f_2(\mathbf{x}) \le 2.8$ $0 \le x_i^{\mathrm{U}}, x_j^{\mathrm{L}} \le 1, \text{ for } i = 1, \cdots, n_{\mathrm{u}}, j = 1, \cdots, K+L$ $s = 1, \beta = 2$
MBOP14	$\min\limits_{\mathbf{x}^{\mathrm{U}}\in\Omega^{\mathrm{U}},\mathbf{x}^{\mathrm{L}}\in\Omega^{\mathrm{L}}} \mathbf{F}(\mathbf{x}^{\mathrm{U}},\mathbf{x}^{\mathrm{L}}) = \begin{pmatrix} f_1(\mathbf{x}) = t_1(\mathbf{x}) + \tau T(t_1(\mathbf{x}), t_2(\mathbf{x})) + \alpha\sum_{j=2}^{K}(x_j^{\mathrm{L}})^2 \\ f_2(\mathbf{x}) = t_2(\mathbf{x}) + \tau T(t_1(\mathbf{x}), t_2(\mathbf{x})) + \alpha\sum_{j=2}^{K}(x_j^{\mathrm{L}})^2 \end{pmatrix}$ subject to $\mathbf{x}^{\mathrm{L}} \in \underset{\mathbf{x}^{\mathrm{L}}\in\Omega^{\mathrm{L}}}{\operatorname{argmin}} \begin{pmatrix} f_1^{\mathrm{L}}(\mathbf{x}) = t_1(\mathbf{x}) + \alpha\big(1 + \sum_{j=2}^{K}(x_j^{\mathrm{L}})^2\big) \\ f_2^{\mathrm{L}}(\mathbf{x}) = t_2(\mathbf{x}) + \alpha\big(1 + \sum_{j=2}^{K}(x_j^{\mathrm{L}})^2\big) \end{pmatrix}$ $t_1(\mathbf{x}) = l(\mathbf{x}^{\mathrm{U}})r(x_1^{\mathrm{L}})\big[\sin(\frac{\pi x_1^{\mathrm{L}}}{2^{s+1}} + (1 + \frac{2^{s-1}}{2^{s+2}})\pi) + 1\big]$ $t_2(\mathbf{x}) = l(\mathbf{x}^{\mathrm{U}})r(x_1^{\mathrm{L}})\big(\cos(\frac{\pi x_1^{\mathrm{L}}}{2} + \pi) + 1\big)$ $l(\mathbf{x}^{\mathrm{U}}) = 1 + \frac{9}{n_{\mathrm{u}}-1}\sum_{i=1}^{n_{\mathrm{u}}} x_i^{\mathrm{U}}$ $r(x_1^{\mathrm{L}}) = 5 + 10(x_1^{\mathrm{L}} - 0.5)^2 + \frac{1}{\beta}\cos(2\beta\pi x_1^{\mathrm{L}}) \times 2^{\frac{s}{2}}$ $T(x_1,x_2) = \begin{cases} 0, if(x_1,x_2) \text{ satisfy } z(x_1,x_2) \\ x_1 + x_2, \text{ otherwise} \end{cases}$ $z(x_1,x_2) = \{(x_1,x_2) \mid (x_1 \in [0.7, 0.83], x_2 \in [4.3, 5]) \cup (x_1 \in [1.05, 1.172], x_2 \in [1.96, 2.44]) \cup (x_1 \in [1.65, 1.77], x_2 \in [0.8, 1.13]) \cup (x_1 \in [2.86, 3.1], x_2 \in [0.142, 0.3])\}$ $0 \le x_i^{\mathrm{U}}, x_j^{\mathrm{L}} \le 1, \text{ for } i = 1, \cdots, n_{\mathrm{u}}, j = 1, \cdots, K$ $\tau = 1, \alpha = 1, s = 1, \beta = 4$
MBOP15	$\min\limits_{\mathbf{x}^{\mathrm{U}}\in\Omega^{\mathrm{U}},\mathbf{x}^{\mathrm{L}}\in\Omega^{\mathrm{L}}} \mathbf{F}(\mathbf{x}^{\mathrm{U}},\mathbf{x}^{\mathrm{L}}) = \begin{pmatrix} f_1(\mathbf{x}) = t_1(\mathbf{x})(1 + \sum_{j=2}^{K}(x_j^{\mathrm{L}})^2) - \tau_1 T(t_1(\mathbf{x}), t_2(\mathbf{x})) \\ f_2(\mathbf{x}) = t_2(\mathbf{x})(1 + \sum_{j=2}^{K}(x_j^{\mathrm{L}})^2) - \tau_1 T(t_1(\mathbf{x}), t_2(\mathbf{x})) \end{pmatrix}$ subject to $\mathbf{x}^{\mathrm{L}} \in \underset{\mathbf{x}^{\mathrm{L}}\in\Omega^{\mathrm{L}}}{\operatorname{argmin}} \begin{pmatrix} f_1^{\mathrm{L}}(\mathbf{x}) = (t_1(\mathbf{x}) + \tau_2(1 + T(t_1(\mathbf{x}), t_2(\mathbf{x}))))(1 + \sum_{j=K+1}^{K+L}(x_j^{\mathrm{L}})^2) \\ f_2^{\mathrm{L}}(\mathbf{x}) = (t_2(\mathbf{x}) + \tau_2(1 + T(t_1(\mathbf{x}), t_2(\mathbf{x}))))(1 + \sum_{j=K+1}^{K+L}(x_j^{\mathrm{L}})^2) \end{pmatrix}$ $t_1(\mathbf{x}) = l(\mathbf{x}^{\mathrm{U}})r(x_1^{\mathrm{L}})\sin\frac{\pi x_1^{\mathrm{L}}}{2}, t_2(\mathbf{x}) = l(\mathbf{x}^{\mathrm{U}})r(x_1^{\mathrm{L}})\cos\frac{\pi x_1^{\mathrm{L}}}{2}$ $r(x_1^{\mathrm{L}}) = 5 + 10(x_1^{\mathrm{L}} - 0.5)^2 + \frac{1}{\beta}\cos(2\beta\pi x_1^{\mathrm{L}})2^{\frac{s}{2}}$ $T(x_1,x_2) = \begin{cases} 0, if(x_1,x_2) \text{ satisfy } z_1(x_1,x_2) \\ 0.5, if(x_1,x_2) \text{ satisfy } z_2(x_1,x_2) \\ 1, \text{otherwise} \end{cases}$ $z_1(x_1,x_2) = \{(x_1,x_2) \mid (x_1 \in [1.13, 1.67], x_2 \in [5.72, 6]) \cup (x_1 \in [2.59, 3], x_2 \in [3.88, 4.15]) \cup (x_1 \in [3.88, 4.24], x_2 \in [2.57, 2.915]) \cup (x_1 \in [5.72, 5.98], x_2 \in [1.15, 1.7])\}$ $z_2(x_1,x_2) = \{(x_1,x_2) \mid (x_1 \in [1.13, 1.67], x_2 \notin [5.72, 6]) \cup (x_1 \in [2.59, 3], x_2 \notin [3.88, 4.15]) \cup (x_1 \in [3.88, 4.24], x_2 \notin [2.57, 2.915]) \cup (x_1 \in [5.72, 5.98], x_2 \notin [1.15, 1.7])\}$ $l(\mathbf{x}^{\mathrm{U}}) = 1 + \sum_{i=1}^{n_{\mathrm{u}}}(x_i^{\mathrm{U}})^{0.1}$ $\mathbf{G}(\mathbf{x}^{\mathrm{U}},\mathbf{x}^{\mathrm{L}}) = f_1(\mathbf{x}) + f_2(\mathbf{x}) \le 8$ $0 \le x_i^{\mathrm{U}}, x_j^{\mathrm{L}} \le 1, \text{ for } i = 1, \cdots, n_{\mathrm{u}}, j = 1, \cdots, K+L$ $\tau_1 = 1, \tau_2 = 5, \beta = 4, s = 1$

TABLE II
CLASSICAL TEST PROBLEM

Test problem	Function
Classic1	$\max\limits_{\mathbf{x}^{\mathrm{U}}\in\Omega^{\mathrm{U}},\mathbf{x}^{\mathrm{L}}\in\Omega^{\mathrm{L}}} \mathbf{F}(\mathbf{x}^{\mathrm{U}},\mathbf{x}^{\mathrm{L}}) = \begin{pmatrix} f_1(\mathbf{x}) = x_1^{\mathrm{U}} + 2x_2^{\mathrm{U}} \\ f_2(\mathbf{x}) = 3x_1^{\mathrm{U}} + x_2^{\mathrm{U}} \end{pmatrix}$ subject to $\mathbf{x}^{\mathrm{L}} \in \operatorname{argmax}\limits_{\mathbf{x}^{\mathrm{L}}\in\Omega^{\mathrm{L}}} \begin{pmatrix} f_1^{\mathrm{L}}(\mathbf{x}) = x_1^{\mathrm{L}} + 3x_2^{\mathrm{L}} \\ f_2^{\mathrm{L}}(\mathbf{x}) = 2x_1^{\mathrm{L}} + x_2^{\mathrm{L}} \end{pmatrix}$ $\mathbf{G}\left(\mathbf{x}^{\mathrm{U}},\mathbf{x}^{\mathrm{L}}\right) = \left\{(x_1^{\mathrm{U}},x_2^{\mathrm{U}}) \in \mathbb{R}^2 \middle\vert x_1^{\mathrm{U}} + \mathbf{x}_2^{\mathrm{U}} \le 3, x_1^{\mathrm{U}}, x_2^{\mathrm{U}} \ge 0\right\}$ $\mathbf{g}\left(\mathbf{x}^{\mathrm{U}},\mathbf{x}^{\mathrm{L}}\right) = \left\{(x_1^{\mathrm{U}},x_2^{\mathrm{U}},x_1^{\mathrm{L}},x_2^{\mathrm{L}}) \in \mathbb{R}^4 \middle\vert -x_1^{\mathrm{U}} + x_1^{\mathrm{L}} + x_2^{\mathrm{L}} \le 6, -x_2^{\mathrm{U}} + x_1^{\mathrm{L}} \le 3, x_1^{\mathrm{U}} + x_2^{\mathrm{U}} + x_2^{\mathrm{L}} \le 8, x_1^{\mathrm{L}}, x_2^{\mathrm{L}} \ge 0\right\}$
Classic2	$\min\limits_{\mathbf{x}^{\mathrm{U}}\in\Omega^{\mathrm{U}},\mathbf{x}^{\mathrm{L}}\in\Omega^{\mathrm{L}}} \mathbf{F}(\mathbf{x}^{\mathrm{U}},\mathbf{x}^{\mathrm{L}}) = \begin{pmatrix} f_1(\mathbf{x}) = x_1^{\mathrm{L}} + (x_2^{\mathrm{L}})^2 + x^{\mathrm{U}} + \sin^2(x_1^{\mathrm{L}} + x^{\mathrm{U}}) \\ f_2(\mathbf{x}) = \cos(x_2^{\mathrm{L}}) \cdot (0.1 + x^{\mathrm{U}}) \cdot (exp(-\frac{x_1^{\mathrm{L}}}{0.1+x_2^{\mathrm{L}}})) \end{pmatrix}$ subject to $\mathbf{x}^{\mathrm{L}} \in \operatorname{argmin}\limits_{\mathbf{x}^{\mathrm{L}}\in\Omega^{\mathrm{L}}} \begin{pmatrix} f_1^{\mathrm{L}}(\mathbf{x}) = \frac{(x_1^{\mathrm{L}}-2)^2+(x_2^{\mathrm{L}}-1)^2}{4} + \frac{x_2^{\mathrm{L}}x^{\mathrm{U}}+(5-x^{\mathrm{U}})^2}{16} + \sin(\frac{x_2^{\mathrm{L}}}{10}) \\ f_2^{\mathrm{L}}(\mathbf{x}) = \frac{(\mathbf{x}_1^{\mathrm{L}})^2+(\mathbf{x}_2^{\mathrm{L}}-6)^4-2\mathbf{x}_1^{\mathrm{L}}\mathbf{x}^{\mathrm{U}}-(5-\mathbf{x}^{\mathrm{U}})^2}{80}) \end{pmatrix}$ $\mathbf{G}\left(\mathbf{x}^{\mathrm{U}},\mathbf{x}^{\mathrm{L}}\right) = \left\{\mathbf{x}^{\mathrm{U}} \in \mathbb{R}^1 \middle\vert 0 \le x^{\mathrm{U}} \le 10\right\}$ $\mathbf{g}\left(\mathbf{x}^{\mathrm{U}},\mathbf{x}^{\mathrm{L}}\right) = \left\{(\mathbf{x}^{\mathrm{U}},\mathbf{x}_1^{\mathrm{L}},\mathbf{x}_2^{\mathrm{L}}) \in \mathbb{R}^3 \middle\vert (x_1^{\mathrm{L}})^2 - x_2^{\mathrm{L}} \le 0, 5(x_1^{\mathrm{L}})^2 + x_2^{\mathrm{L}} \le 10, x_2^{\mathrm{L}} - (5 - x^{\mathrm{U}}/6) \le 0, x_1^{\mathrm{L}} \ge 0\right\}$

TABLE III
MATHEMATICAL DEFINITIONS OF THE PETROLEUM REFINING MBLOP

Petroleum Refining MBLOP	Function
Objective	$\min\limits_{\tau\in\Omega^{\mathrm{U}},F^c,\mathbf{F}^p,F^s\in\Omega^{\mathrm{L}}} \mathbf{F}(\tau,F^c,\mathbf{F}^p,F^s) = \begin{pmatrix} f_1(\mathbf{x}) = Q^{\mathrm{fue}}\zeta \\ f_2(\mathbf{x}) = -\sum_{i=1}^{n^p}\tau_i F_i^p \end{pmatrix}$ subject to $(F^c,\mathbf{F}^p,F^s) \in \operatorname{argmin}$ $\left(f_1^{\mathrm{L}}(\mathbf{x}) = -\sum_{i=1}^{n^p} C_i^p F_i^p + C^c F^c + C^s F^s + \left(\sum_{i=1}^{n^p}\tau_i F_i^p\right) \& f_2^{\mathrm{L}}(\mathbf{x}) = Q^{\mathrm{fue}} \right)$
Constraint	Upper Level: $f_1(\mathbf{x}) \ge 0$, $f_2(\mathbf{x}) \le 0$ Lower Level: $F^c - \sum_{i=1}^{n^p} F_i^p \ge 0$, $f_2^{\mathrm{L}}(\mathbf{x}) \ge 0$
Variable	Upper Level:$1.0 \le \tau_1 \le 1.4$, $0.6 \le \tau_2 \le 1.0$, $0.6 \le \tau_3 \le 1.0$, $0.6 \le \tau_4 \le 1.0$ Lower Level:$10.1 \le F_1^p \le 10.21$, $30.01 \le F_2^p \le 30.93$ $59.6 \le F_3^p \le 60.5$, $26.84 \le F_4^p \le 31.52$, $448.52 \le F^c \le 458.45$, $0.35 \le F^s \le 0.36$
Related Calculations	$Q^{\mathrm{fue}} = Q^{\mathrm{fst}} + Q^{\mathrm{fur}} = \frac{Q^{\mathrm{pst}}}{\lambda^p}(h^p - h^w)\frac{T^{\mathrm{ftb}}-T^0}{T^{\mathrm{ftb}}-T^s} + \frac{Q^{\mathrm{pfu}}}{\eta^f}$ $\eta^f = \frac{T^{\mathrm{ftf}}-T^s}{T^{\mathrm{ftf}}-T^0}$ $\zeta = \left(\frac{\alpha}{\phi}\right)\left(\frac{C\%}{100}\right)$ $Q^{\mathrm{pst}} = \beta F^s$ $Q^{\mathrm{pfu}} = \gamma\left(F^c + \sum_{i=1}^{n^p} F_i^p\right)$

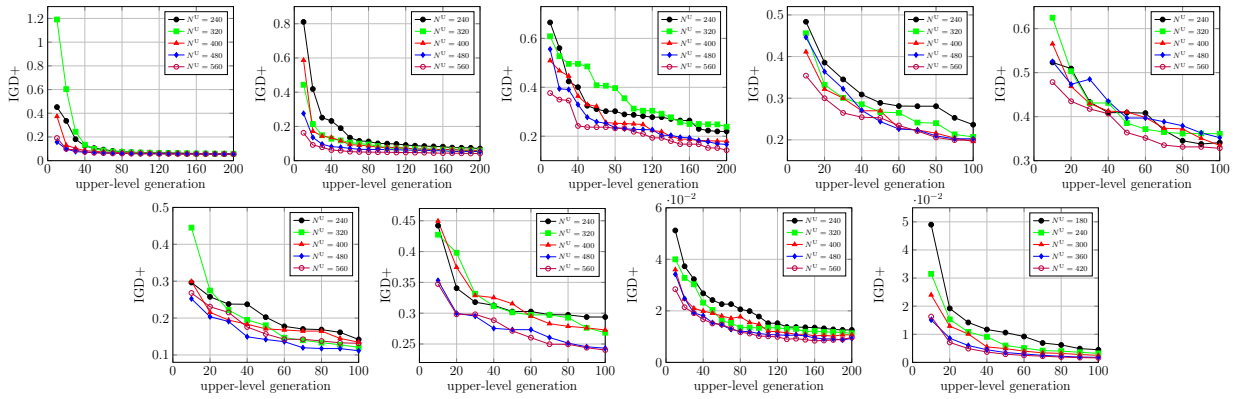

Fig. 29. Influence of the hyperparameter N^{U} on the convergence measuring by IGD+.

TABLE IV
SUMMARY OF NOTATIONS USED IN THE PRACTICAL PETROLEUM REFINING MULTIOBJECTIVE BILEVEL PROBLEM

Parameter	Description	Value
ζ	the relevant fuel factor	—
n^p	the number of oil products	4
λ^p, h^p	the latent heat and enthalpy of steam	1933.19, 2791.73
Q^{pst}	the heat duty required by steam heating	—
Q^{pfu}	the heat duty required by furnace	—
h^w	the enthalpy of the boiler feed water at 100°C	419
T^{ftb}	the flame temperature of the boiler flue gas	1800
T^0	the environmental temperature	25
T^s	the stack temperature of exhaust gas	160
T^{ftf}	the theoretical flame temperature of the furnace	1800
η^f	the theoretical efficiency of the furnace	—
α	the ratio of molar masses of CO_2 and C	3.67
C%	carbon content	0.865
ϕ	the net heating value of fuel with a carbon content of C%	3971
τ_i	per unit tax imposed on the oil product i. $(i = 1, \ldots, n^p)$	—
F^c, F^s, F_i^p	the flow rate of crude oil, steam, product i. $(i = 1, \ldots, n^p)$	—
C^c, C^s, C_i^p	the prices of crude, steam, product i. $(i = 1, \ldots, n^p)$	79.6, 0.14, 103.5, 92.7, 99.0, 96.6
Q^{fue}	the amount of fuel burnt for the crude oil distillation process	—
Q^{fst}, Q^{fur}	the amount of fuel burnt for the steam boilers and furnace	—
γ	the ratio of the heat duty required by the furnace and the yield of the crude oil and product flow rate	1
β	the ratio of the steam heat duty and the steam flow rate	1

TABLE V
PARAMETER SETTING

Test problem	N^{U}	T^{U}	N^{L}	T^{L}	Variable dimension	Ideal point	Nadir point
MBOP1	400	200	40	40	(K, K)	(0, 0)	(1.1, 1.1)
MBOP2	400	200	40	40	(K, K)	(-0.2388, -0.8378)	(0.8090, 0.0138)
MBOP3	400	200	40	40	(K, K)	(-0.1882, -0.2427)	(1.4, 1)
MBOP4	400	100	40	40	(1, K+L)	(0, 0)	(1, 2)
MBOP5	400	100	40	40	(1, K+L)	(0, 0)	(1, 1.8)
MBOP6	400	100	40	40	(1, K+L)	(0, 0)	(1, 2)
MBOP7	400	100	40	40	(1, K+L)	(0, 0)	(1, 1.8)
MBOP8	400	200	40	40	(1, 2)	(-2, -1)	(-1, 0)
MBOP9	300	100	60	80	(1, K)	(0.5, 0)	(1, 0.5)
MBOP10	600	200	60	40	(1, 2)	(23, 2)	(2, -9)
MBOP11	400	200	40	100	(2, 3)	(-300, -2000)	(-1200, -300)
MBOP12	400	200	40	40	(K, K)	(0, 0)	(1.1, 1.1)
MBOP13	400	200	40	40	(n_{u}, $K + L$)	(0.0436, 0.9)	(2.073, 3.433)
MBOP14	400	100	40	40	(n_{u}, K)	(0.7052, 0.1427)	(3.0957, 4.9934)
MBOP15	400	200	40	60	(n_{u}, $K + L$)	(1.1340,1.1534)	(5.971, 5.9958)
Classic1	200	50	40	40	(2, 2)	(-6,-9)	(-3, -3)
Classic2	200	50	40	40	(1, 2)	(23,2)	(2, -9)
Petroleum Refining	400	50	40	40	(4, 6)	(4.9×10^{-4}, -138)	(5.1×10^{-4}, -80)

TABLE VI
MEDIAN AND INTERQUARTILE RANGE OF IGD, HV AND IGD+ ON MBOP TEST PROBLEMS.

Test Problem	TKDEA			BLEMO			OMOPSO-BL		
	IGD	HV	IGD+	IGD	HV	IGD+	IGD	HV	IGD+
MBOP1	**5.85E-2**	**7.21E-1**	**5.66E-2**	1.77E+0†	0.00E+0†	1.75E+0†	1.87E-1†	5.37E-1†	1.70E-1†
	1.73E-3	**2.81E-3**	**1.35E-3**	2.31E+0	2.18E-2	2.32E+0	8.71E-2	9.67E-2	9.95E-2
MBOP2	**4.87E-2**	**5.12E-1**	**4.85E-2**	3.48E+0†	0.00E+0†	3.48E+0†	3.40E-1†	1.40E-1†	3.40E-1†
	7.94E-3	**1.64E-2**	**8.23E-3**	4.15E+0	0.00E+0	4.17E+0	1.86E-1	9.35E-2	1.92E-1
MBOP3	**1.57E-1**	**4.12E-1**	**1.54E-1**	8.16E-1†	6.77E-2†	7.91E-1†	1.51E+0†	0.00E+0†	1.51E+0†
	8.87E-2	**9.42E-2**	**8.15E-2**	6.18E-1	1.34E-1	6.32E-1	3.89E-1	0.00E+0	3.89E-1
MBOP4	2.06E-1	2.53E-1	1.89E-1	1.81E-1≈	3.47E-1‡	1.65E-1‡	**3.32E-2‡**	**4.61E-1‡**	**3.06E-2‡**
	7.02E-2	6.45E-2	6.57E-2	9.24E-2	4.90E-2	6.31E-2	**8.45E-3**	**8.04E-3**	**7.39E-3**
MBOP5	3.70E-1	1.13E-1	3.24E-1	3.96E-1≈	1.83E-1‡	3.05E-1≈	**2.27E-1‡**	**2.61E-1‡**	**2.06E-1‡**
	6.51E-2	4.27E-2	5.35E-2	1.44E-1	2.12E-2	6.26E-2	**9.65E-3**	**9.12E-3**	**8.98E-3**
MBOP6	**1.49E-1**	3.22E-1	**1.35E-1**	1.89E-1≈	**3.52E-1**≈	1.45E-1≈	3.11E-1†	2.28E-1†	3.09E-1†
	3.45E-2	4.00E-2	**3.28E-2**	1.31E-1	**7.50E-2**	8.02E-2	4.64E-2	3.22E-2	4.68E-2
MBOP7	**2.81E-1**	1.87E-1	**2.64E-1**	3.65E-1†	**2.00E-1**≈	2.88E-1†	6.46E-1†	7.26E-3†	6.28E-1†
	2.67E-2	3.30E-2	**2.85E-2**	1.81E-1	**4.72E-2**	7.86E-2	1.63E-1	4.11E-2	1.50E-1
MBOP8	9.94E-2	7.60E-3	**1.11E-3**	**4.94E-2‡**	**2.14E-1‡**	1.13E-2†	8.75E-2†	9.54E-3≈	1.35E-3≈
	1.33E-2	4.05E-2	**1.88E-3**	**2.68E-2**	**5.45E-2**	1.13E-2	5.79E-3	2.12E-2	8.11E-4
MBOP9-K2	**4.05E-3**	**8.18E-1**	**2.35E-3**	1.47E-1†	2.89E-1†	8.18E-2†	1.93E-2†	7.29E-1†	5.68E-3†
	6.54E-4	**2.81E-3**	**3.73E-4**	1.12E-1	5.38E-1	1.10E-1	1.09E-2	7.78E-2	3.38E-3
MBOP9-K6	**6.31E-3**	**8.09E-1**	**2.99E-3**	1.30E-1†	5.06E-1†	7.29E-2†	2.79E-2†	7.08E-1†	5.69E-3†
	1.38E-3	**5.82E-3**	**7.83E-4**	1.33E-1	3.85E-1	7.47E-2	1.59E-2	1.57E-1	5.14E-3
MBOP9-K14	**1.85E-2**	**7.76E-1**	8.16E-3	1.78E-1†	4.09E-1†	1.32E-1†	2.91E-2†	7.54E-1†	**6.31E-3‡**
	7.00E-3	**2.73E-2**	2.50E-3	3.10E-1	5.24E-1	3.16E-1	1.40E-2	6.24E-2	**2.91E-3**
MBOP10	-	4.11E-1	-	-	3.85E-1†	-	-	**5.08E-1‡**	-
	-	1.58E-2	-	-	9.29E-3	-	-	**8.85E-3**	-
MBOP11	-	**7.19E-1**	-	-	3.44E-1†	-	-	6.82E-1†	-
	-	**3.72E-1**	-	-	2.94E-1	-	-	1.22E-1	-
MBOP12	**4.63E-3**	**7.79E-1**	**4.04E-3**	1.25E+0†	0.00E+0†	1.21E+0†	1.79E-1†	5.23E-1†	1.70E-1†
	1.15E-3	**1.36E-3**	**9.38E-4**	1.06E+0	3.74E-2	1.09E+0	4.37E-2	7.86E-2	5.95E-2
MBOP13	**8.10E-2**	**6.18E-1**	**3.28E-2**	9.09E-1†	2.36E-1†	9.04E-1†	7.32E+0†	0.00E+0†	7.30E+0†
	1.89E-2	**5.64E-3**	**6.43E-3**	1.25E+0	4.45E-1	1.27E+0	2.26E+0	0.00E+0	2.29E+0
MBOP14	**8.74E-1**	**6.75E-1**	**2.21E-1**	1.59E+1†	0.00E+0†	1.59E+1†	1.11E+1†	0.00E+0†	1.11E+1†
	1.06E-3	**5.99E-5**	**5.62E-5**	1.14E+1	0.00E+0	1.14E+1	3.58E+0	0.00E+0	3.58E+0
MBOP15	**3.16E-2**	**4.44E-1**	**2.56E-2**	8.75E-2≈	4.25E-1≈	8.55E-2≈	1.36E+1†	0.00E+0†	1.36E+1†
	8.64E-3	**1.72E-3**	**5.80E-3**	-	-	-	5.96E-1	0.00E+0	5.96E-1
†/≈/‡				10/4/1	11/3/3	11/3/1	13/0/2	13/1/3	11/1/3

† denotes the performance of TKDEA is significantly better than the other peers according to the Wilcoxon signed-rank test at a 0.05 significance level while ‡ denotes the opposite case, and ≈ denotes that there is no significant difference between the two algorithms.
The IGD and IGD+ values of MBOP10 and MBOP11 are not available due to the lack of their true PF.

TABLE VII
THE NONDOMINATED SOLUTIONS OF MBOP11

	$\mathbf{x}^{\mathrm{U}}$	$\mathbf{x}^{\mathrm{L}}$	$f_1(\mathbf{x})$	$f_2(\mathbf{x})$	$f_1^{\mathrm{L}}(\mathbf{x})$	$f_2^{\mathrm{L}}(\mathbf{x})$
Solution given in [13]	(146.2955, 28.9394)	(0, 67.9318, 0)	474.6819	1850.0609	1030.5456	1469.0532
Solution A	(0.5600, 107.5164)	(0, 0, 23.2238)	1037.8790	312.9680	833.1288	526.3208
Solution B	(16.6666, 100)	(0, 0, 29.6665)	1005.6661	468.6654	903.9984	618.6656
Solution C	(92.9000, 64.4244)	(0, 0, 60.1598)	853.1990	1205.5880	1239.4248	1055.7368
Solution D	(146.1023, 29.0719)	(0, 67.6585, 0.2501)	476.1582	1847.6744	1031.4754	1467.5113

TABLE VIII
MEAN AND STANDARD DEVIATION OF THE NUMBER OF FUNCTION EVALUATIONS ON MBOP TEST PROBLEMS

Test Problem	TKDEA/ BLEMO			OMOPSO-BL		
	FE	ULFE	LLFE	FE	ULFE	LLFE
MBOP1	3296400(0)	80400(0)	3216000(0)	3531820(17902)	162620(437)	3369200(17465)
MBOP2	3296400(0)	80400(0)	3216000(0)	3517306(13753)	162266(335)	3355040(13418)
MBOP3	3296400(0)	80400(0)	3216000(0)	3856294(40817)	170534(996)	3685760(39821)
MBOP4	1656400(0)	40400(0)	1616000(0)	2143950(63960)	90720(1560)	2053200(62400)
MBOP5	1656400(0)	40400(0)	1616000(0)	1996320(54120)	87120(1320)	1909200(52800)
MBOP6	1656400(0)	40400(0)	1616000(0)	1928588(27599)	85468(673)	1843120(26926)
MBOP7	1656400(0)	40400(0)	1616000(0)	2049620(37622)	88420(918)	1961200(36704)
MBOP8	3296400(0)	80400(0)	3216000(0)	3700904(43292)	166744(1056)	3534160(42236)
MBOP9-K2	2454300(0)	30300(0)	2424000(0)	2857530(54651)	64830(675)	2792700(53976)
MBOP9-K6	2454300(0)	30300(0)	2424000(0)	2874297(56666)	65037(700)	2809260(55966)
MBOP9-K14	2454300(0)	30300(0)	2424000(0)	2907588(49672)	65448(613)	2842140(49059)
MBOP10	4944600(0)	120600(0)	4824000(0)	5827860(87945)	256860(2145)	5571000(85800)
MBOP11	8120400(0)	80400(0)	8040000(0)	8802360(116150)	165960(1150)	8636400(115000)
MBOP12	3296400(0)	80400(0)	3216000(0)	3524932(15429)	162452(376)	3362480(15053)
MBOP13	1656400(0)	40400(0)	1616000(0)	1789024(14516)	82064(354)	1706960(14162)
MBOP14	1648200(0)	40200(0)	1608000(0)	1754430(5311)	81030(130)	1673400(5182)
MBOP15	828200(0)	20200(0)	808000(0)	1043178(24482)	44658(597)	998520(23885)

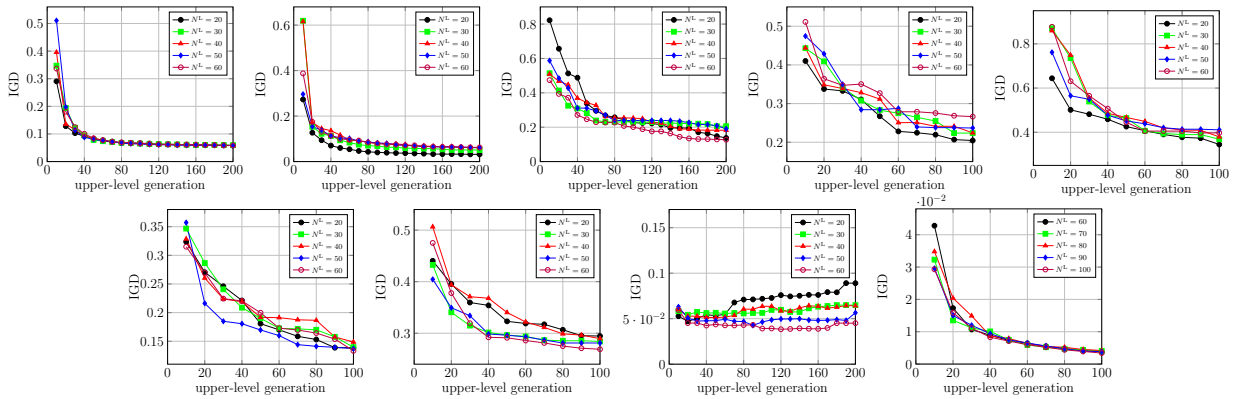

Fig. 30. Influence of the hyperparameter N^{L} on the convergence measuring by IGD.

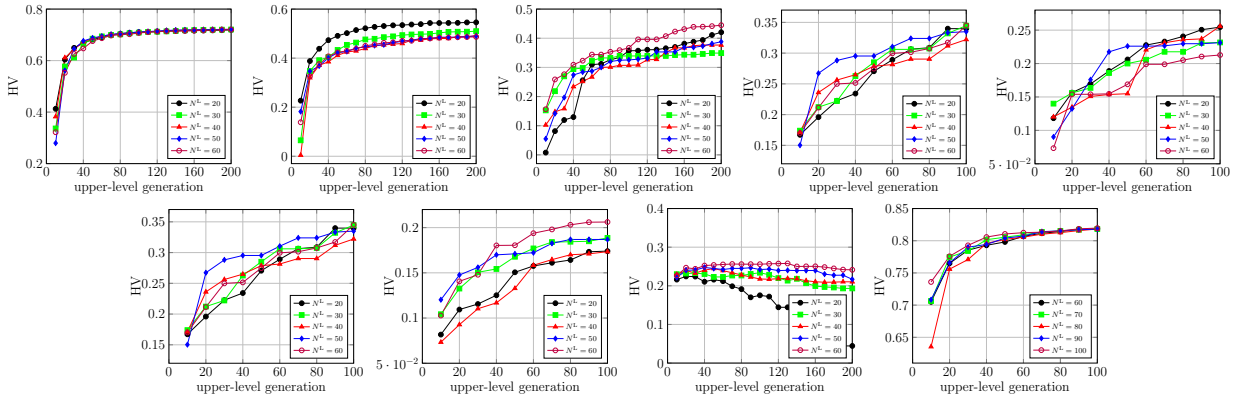

Fig. 31. Influence of the hyperparameter N^{L} on the convergence measuring by HV.

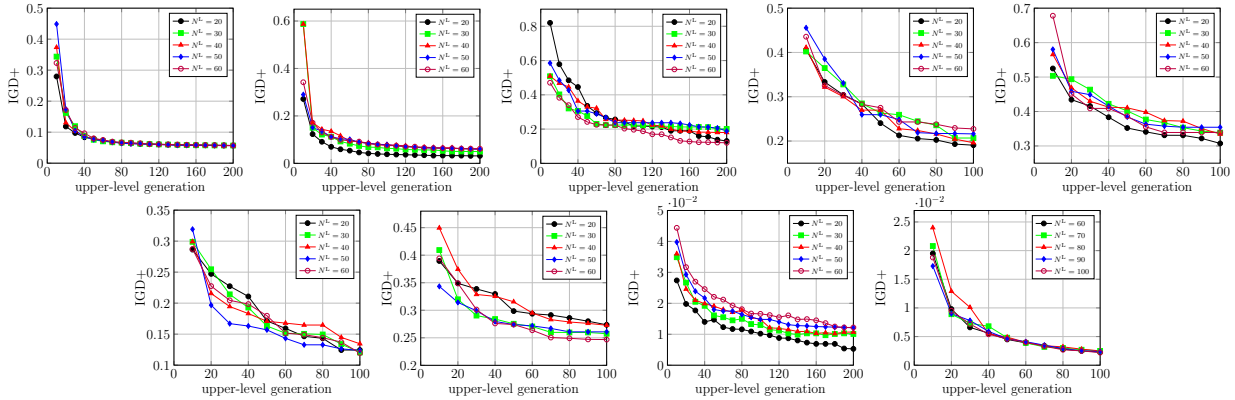

Fig. 32. Influence of the hyperparameter N^{L} on the convergence measuring by IGD+.

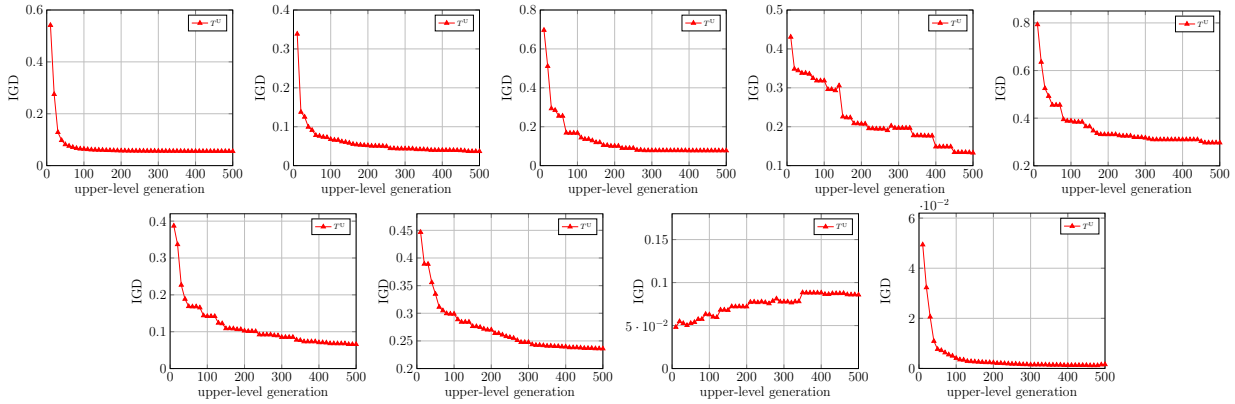

Fig. 33. Influence of the hyperparameter T^{U} on the convergence measuring by IGD.

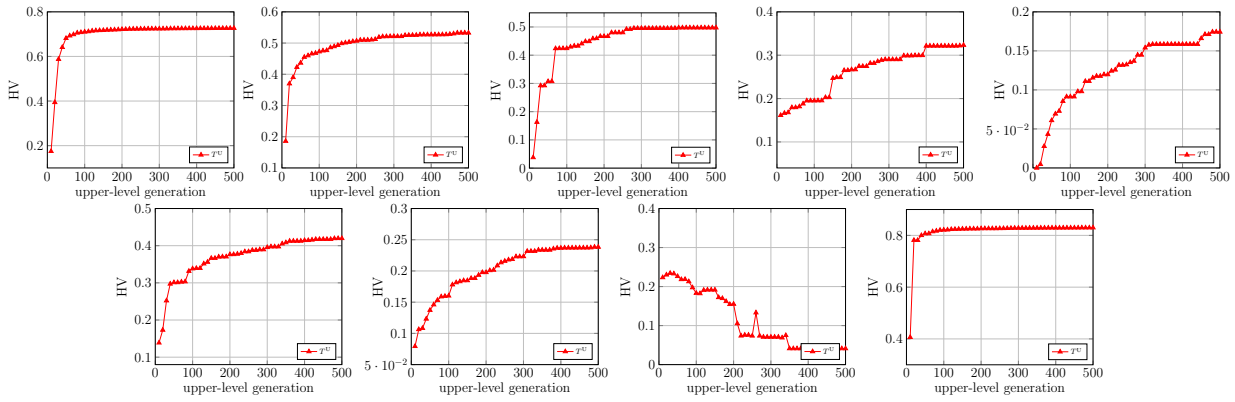

Fig. 34. Influence of the hyperparameter T^{U} on the convergence measuring by HV.

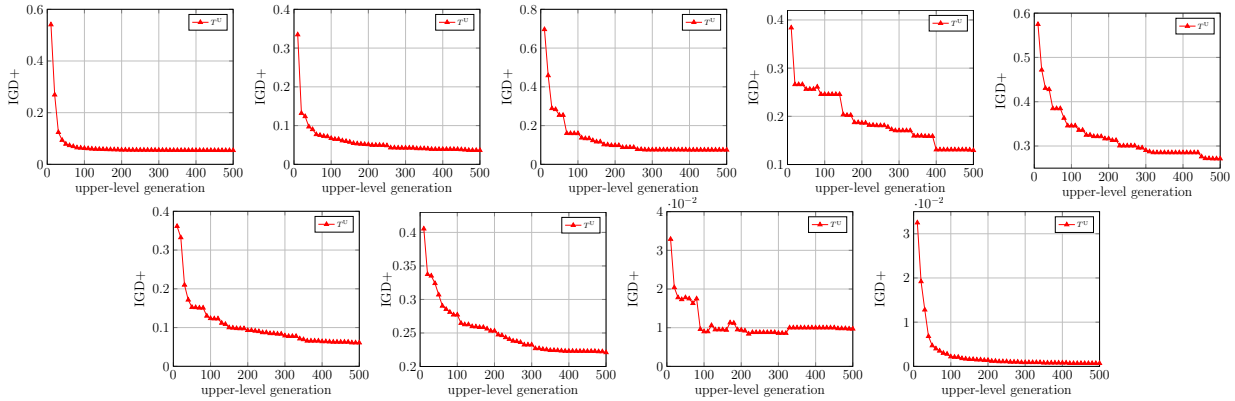

Fig. 35. Influence of the hyperparameter T^{U} on the convergence measuring by IGD+.

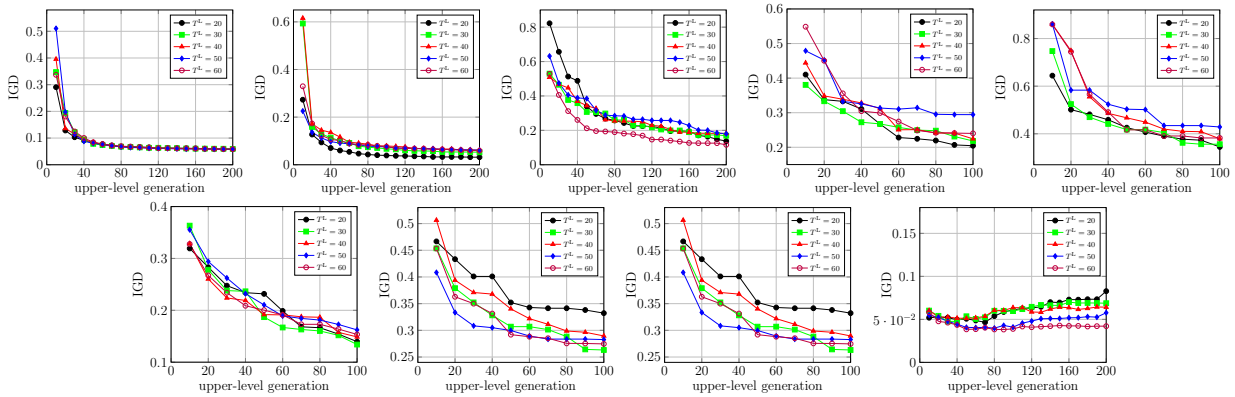

Fig. 36. Influence of the hyperparameter T^{L} on the convergence measuring by IGD.

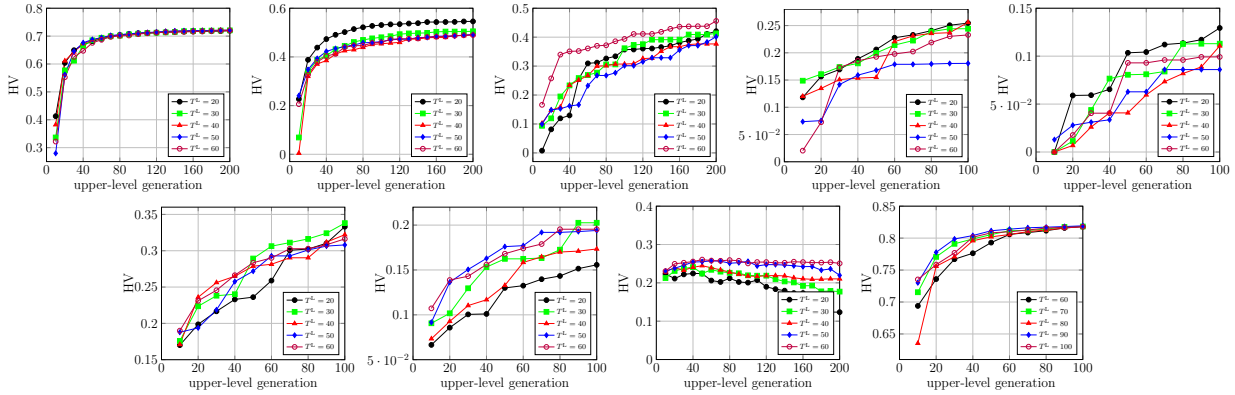

Fig. 37. Influence of the hyperparameter T^{L} on the convergence measuring by HV.

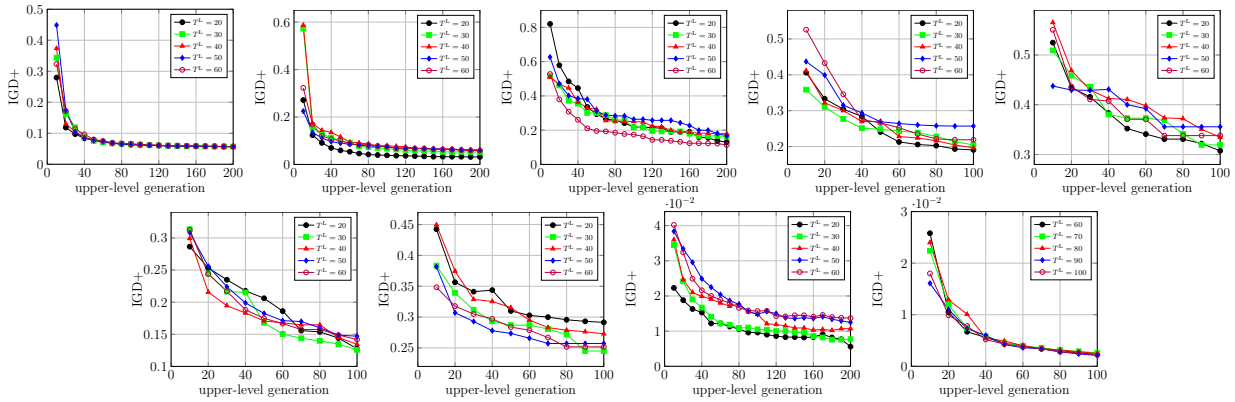

Fig. 38. Influence of the hyperparameter T^{L} on the convergence measuring by IGD+.

TABLE IX
MEDIAN AND IQR OF HV ON CLASSICAL1

HV	TKDEA	CA1	CA2
Classic1	**4.84E-1 (9.73E-3)**	4.08E-1† (0.00E+0)	2.50E-1† (0.00E+0)

† denotes the performance of TKDEA is significantly better than the other peers according to the Wilcoxon signed-rank test at a 0.05 significance level.

TABLE X
MEDIAN AND IQR OF HV ON CLASSICAL2

HV	TKDEA	CA3
Classic2	**5.11E-1 (1.20E-2)**	4.61E-1† (0.00E+0)

† denotes the performance of TKDEA is significantly better than the other peers according to the Wilcoxon signed-rank test at a 0.05 significance level.

TABLE XI
MEDIAN AND IQR OF HV AND THE NUMBER OF FUNCTION EVALUATIONS ON PRACTICAL REFINING PROBLEM

	TKDEA	BLEMO	OMOPSO-BL
HV	**6.16E-1 (1.08E-4)**	5.58E-1† (1.09E-1)	5.44E-1† (2.77E-2)
FE	836400 (0.00E+0)	836400 (0.00E+0)	946080 (1.80E+4)
ULFE	20400 (0.00E+0)	20400 (0.00E+0)	42480 (4.40E+2)
LLFE	816000 (0.00E+0)	816000 (0.00E+0)	903600 (1.76E+4)

† indicates that TKDEA outperforms its peers using the Wilcoxon signed-rank test at a significance level of 0.05.

TABLE XII
MEDIAN AND INTERQUARTILE RANGE OF IGD, HV AND IGD+ ON MBOP TEST PROBLEMS.

Test Problem	Indicator	TKDEA	B-C-TAEA	B-I-DBEA	B-DMOEA-εC
MBOP1	IGD	**5.85E-2(1.73E-3)**	5.97E-2(3.98E-3)†	5.95E-2(4.74E-3)≈	6.01E-2(5.36E-3)†
	HV	**7.21E-1(2.81E-3)**	7.19E-1(3.34E-3)≈	7.17E-1(4.52E-3)†	7.20E-1(6.81E-3)≈
	IGD+	5.66E-2(1.35E-3)	5.73E-2(2.12E-3)≈	5.73E-2(4.36E-3)≈	**5.63E-2(3.94E-3)**≈
MBOP2	IGD	4.87E-2(7.94E-3)	**2.54E-2(5.24E-3)**‡	3.39E-2(7.48E-3)‡	2.87E-2(6.45E-3)‡
	HV	5.12E-1(1.64E-2)	**5.57E-1(1.02E-2)**‡	5.42E-1(1.30E-2)‡	5.53E-1(1.10E-2)‡
	IGD+	4.85E-2(8.23E-3)	**2.51E-2(5.25E-3)**‡	3.35E-2(7.40E-3)‡	2.82E-2(6.40E-3)‡
MBOP3	IGD	**1.57E-1(8.87E-2)**	2.45E-1(3.12E-1)†	2.35E-1(2.07E-1)†	NaN†
	HV	**4.12E-1(9.42E-2)**	3.71E-1(2.57E-1)†	3.38E-1(1.23E-1)†	NaN†
	IGD+	**1.54E-1(8.15E-2)**	2.33E-1(3.06E-1)†	2.33E-1(1.77E-1)†	NaN†
MBOP4	IGD	2.06E-1(7.02E-2)	1.63E-1(2.46E-2)‡	**1.50E-1(4.02E-2)**‡	2.00E-1(5.38E-2)≈
	HV	2.53E-1(6.45E-2)	3.08E-1(4.48E-2)‡	**3.16E-1(3.72E-2)**‡	2.67E-1(6.01E-2)≈
	IGD+	1.89E-1(6.57E-2)	1.52E-1(3.16E-2)‡	**1.41E-1(3.62E-2)**‡	1.86E-1(4.77E-2)≈
MBOP5	IGD	3.70E-1(6.51E-2)	3.16E-1(4.13E-2)‡	**3.07E-1(3.00E-2)**‡	3.53E-1(5.25E-2)≈
	HV	1.13E-1(4.27E-2)	1.51E-1(4.04E-2)‡	**1.59E-1(2.98E-2)**‡	1.21E-1(4.19E-2)≈
	IGD+	3.24E-1(5.35E-2)	2.92E-1(3.69E-2)≈	**2.86E-1(2.93E-2)**‡	3.21E-1(3.92E-2)≈
MBOP6	IGD	1.49E-1(3.45E-2)	**1.42E-1(2.60E-2)**≈	1.61E-1(3.87E-2)≈	1.84E-1(4.77E-2)†
	HV	3.22E-1(4.00E-2)	3.22E-1(3.49E-2)≈	**3.29E-1(5.46E-2)**≈	2.85E-1(3.79E-2)†
	IGD+	1.35E-1(3.28E-2)	**1.34E-1(2.66E-2)**≈	1.47E-1(3.66E-2)≈	1.73E-1(4.40E-2)†
MBOP7	IGD	**2.81E-1(2.67E-2)**	2.95E-1(3.02E-2)≈	3.06E-1(5.73E-2)†	3.48E-1(4.21E-2)†
	HV	**1.87E-1(3.30E-2)**	1.64E-1(3.47E-2)†	1.80E-1(2.66E-2)≈	1.30E-1(3.78E-2)‡
	IGD+	**2.64E-1(2.85E-2)**	2.84E-1(3.17E-2)≈	2.85E-1(4.83E-2)†	3.14E-1(3.37E-2)†
MBOP8	IGD	**9.94E-2(1.33E-2)**	1.09E-1(1.25E-2)≈	1.14E-1(3.93E-3)†	8.18E-1(3.95E-1)†
	HV	**7.60E-3(4.05E-2)**	0.00E+0(1.12E-3)†	0.00E+0(1.68E-3)†	0.00E+0(0.00E+0)≈
	IGD+	1.11E-3(1.88E-3)	2.75E-4(2.01E-3)‡	**2.67E-5(4.61E-5)**‡	5.70E-1(4.27E-1)†
MBOP9-K2	IGD	**4.05E-3(6.54E-4)**	4.31E-3(1.01E-3)†	6.97E-3(1.64E-3)†	4.70E-3(1.58E-3)†
	HV	**8.18E-1(2.81E-3)**	8.16E-1(5.01E-3)†	8.05E-1(6.75E-3)†	8.17E-1(4.60E-3)≈
	IGD+	**2.35E-3(3.73E-4)**	2.47E-3(4.27E-4)≈	3.22E-3(5.07E-4)†	2.62E-3(5.63E-4)†
MBOP9-K6	IGD	**6.31E-3(1.38E-3)**	1.07E-2(2.22E-3)†	3.31E-2(2.53E-2)†	2.93E-2(3.29E-2)≈
	HV	**8.09E-1(5.82E-3)**	7.78E-1(4.11E-2)†	7.08E-1(1.61E-1)†	7.45E-1(6.88E-2)†
	IGD+	**2.99E-3(7.83E-4)**	3.73E-3(1.14E-3)†	1.11E-2(5.03E-3)†	6.20E-3(5.57E-3)†
MBOP9-K14	IGD	**1.85E-2(7.00E-3)**	3.75E-2(1.33E-2)†	2.30E-1(1.27E-1)†	5.26E-2(2.57E-2)†
	HV	**7.76E-1(2.73E-2)**	6.96E-1(4.38E-2)†	1.44E-1(2.01E-1)†	6.87E-1(5.89E-2)†
	IGD+	**8.16E-3(2.50E-3)**	1.83E-2(7.60E-3)†	2.18E-1(1.41E-1)†	2.48E-2(1.20E-2)†
MBOP10	IGD	-	-	-	-
	HV	4.11E-1(1.58E-2)	**5.51E-1(3.21E-3)**‡	5.19E-1(1.66E-2)‡	1.08E-1(4.74E-2)≈
	IGD+	-	-	-	-
MBOP11	IGD	-	-	-	-
	HV	7.19E-1(3.72E-1)	6.11E-1(3.24E-1)†	5.59E-1(1.63E-1)†	**7.28E-1(8.40E-2)**≈
	IGD+	-	-	-	-
†/≈/‡			15/10/10	18/6/11	18/13/4

† denotes the performance of TKDEA is significantly better than the other peers according to the Wilcoxon signed-rank test at a 0.05 significance level while ‡ denotes the opposite case, and ≈ denotes that there is no significant difference between the two algorithms.
The IGD and IGD+ values of MBOP10 and MBOP11 are not available due to the lack of their true PF.

TABLE XIII
HYPERPARAMETER SETTING

	p_m	N^{U}	N^{L}	T^{L}
MBLOP1	$\{\frac{1}{n_\ell+2},\frac{1}{n_\ell+1},\frac{1}{n_\ell},\frac{1}{n_\ell-1},\frac{1}{n_\ell-2}\}$	{240, 320, 400, 480, 560}	{20, 30, 40, 50, 60}	{20, 30, 40, 50, 60 }
MBLOP2	$\{\frac{1}{n_\ell+2},\frac{1}{n_\ell+1},\frac{1}{n_\ell},\frac{1}{n_\ell-1},\frac{1}{n_\ell-2}\}$	{240, 320, 400, 480, 560}	{20, 30, 40, 50, 60}	{20, 30, 40, 50, 60 }
MBLOP3	$\{\frac{1}{n_\ell+2},\frac{1}{n_\ell+1},\frac{1}{n_\ell},\frac{1}{n_\ell-1},\frac{1}{n_\ell-2}\}$	{240, 320, 400, 480, 560}	{20, 30, 40, 50, 60}	{20, 30, 40, 50, 60 }
MBLOP4	$\{\frac{1}{n_\ell+4},\frac{1}{n_\ell+3},\frac{1}{n_\ell+2},\frac{1}{n_\ell+1},\frac{1}{n_\ell}\}$	{240, 320, 400, 480, 560}	{20, 30, 40, 50, 60}	{20, 30, 40, 50, 60 }
MBLOP5	$\{\frac{1}{n_\ell+4},\frac{1}{n_\ell+3},\frac{1}{n_\ell+2},\frac{1}{n_\ell+1},\frac{1}{n_\ell}\}$	{240, 320, 400, 480, 560}	{20, 30, 40, 50, 60}	{20, 30, 40, 50, 60 }
MBLOP6	$\{\frac{1}{n_\ell+4},\frac{1}{n_\ell+3},\frac{1}{n_\ell+2},\frac{1}{n_\ell+1},\frac{1}{n_\ell}\}$	{240, 320, 400, 480, 560}	{20, 30, 40, 50, 60}	{20, 30, 40, 50, 60 }
MBLOP7	$\{\frac{1}{n_\ell+4},\frac{1}{n_\ell+3},\frac{1}{n_\ell+2},\frac{1}{n_\ell+1},\frac{1}{n_\ell}\}$	{240, 320, 400, 480, 560}	{20, 30, 40, 50, 60}	{20, 30, 40, 50, 60 }
MBLOP8	$\{\frac{1}{n_\ell+4},\frac{1}{n_\ell+3},\frac{1}{n_\ell+2},\frac{1}{n_\ell+1},\frac{1}{n_\ell}\}$	{240, 320, 400, 480, 560}	{20, 30, 40, 50, 60}	{20, 30, 40, 50, 60 }
MBLOP9	$\{\frac{1}{n_\ell+4},\frac{1}{n_\ell+3},\frac{1}{n_\ell+2},\frac{1}{n_\ell+1},\frac{1}{n_\ell}\}$	{180, 240, 300, 360, 420}	{60, 70, 80, 90, 100}	{60, 70, 80, 90, 100}